Fakultät für Medizin
Urologische Klinik und Poliklinik

Identification of molecular mechanisms induced by CDK4/6 inhibition

Qi Pan

Vollständiger Abdruck der von der Fakultät für Medizin der Technischen Universität München zur Erlangung des akademischen Grades eines
Doktors der Medizin
genehmigten Dissertation.

Vorsitzender: Prof. Dr. Jürgen Schlegel
Prüfer der Dissertation:
1: Prof. Dr. Jürgen Gschwend
2: Prof. Dr. Roland M. Schmid

Die Dissertation wurde am 19.03.2018 bei der Fakultät für Medizin der Technischen Universität München eingereicht und durch die Fakultät für Medizin am 13.11.2018 angenommen.

AFFIDAVIT

I hereby declare that the dissertation titled

Identification of molecular mechanisms induced by CDK4/6 inhibition prepared under the guidance and supervision of Univ.-Prof. Dr. Jürgen E. Gschwend at the Department of Urology

and submitted to the degree-awarding institution of: The Faculty of Medicine of TUM is my own, original work undertaken in partial fulfillment of the requirements for the doctoral degree. I have made no use of sources, materials or assistance other than those specified in § 6 (6) and (7), clause 2.

[X] I have not employed the services of an organization that provides dissertation supervisors in return for payment or that fulfills, in whole or in part, the obligations incumbent on me in connection with my dissertation.

[X] I have not submitted the dissertation, either in the present or a similar form, as part of another examination process.

[ ] The complete dissertation was published in _____

the degree-awarding institution: _____

has approved prior publication of the dissertation.

[X] I have not yet been awarded the desired doctoral degree nor have I failed the last possible attempt to obtain the desired degree in a previous doctoral program.

[ ] I have already applied for admission to a doctoral program at the school or college of

_____

at (university) _____

by submitting a dissertation on the topic _____

With the result: _____

I am familiar with the publicly available Regulations of the Award of Doctoral Degrees of TUM, in particular § 28 (Invalidation of doctoral degree) and § 29 (Revocation of doctoral degree). I am aware of the consequences of filling a false affidavit.

[X] I agree [ ] I do not agree

that my personal data is stored in the TUM alumni database.

Munich, 5.3.2018 PAN Qi 潘麒

Abstract

The CDK4/6-RB1-E2F pathway, which regulates the transition of cell cycle from G1 to S phase, is frequently disrupted in advanced bladder cancer (BC). Our previous work has characterized this pathway as a potential therapy target using CDK4/6 inhibitors. In this project, we further studied molecular mechanisms induced by CDK4/6 inhibitor (PD-0332991) and their implication on therapy response in BC. A prerequisite for response to CDK4/6 inhibitors is the expression of RB1, since RB1-negative cells, which are either RB1 mutant or established via RB1 knockdown, were non-responsive to treatment. On the other hand, therapy response of RB1 positive cells to PD-0332991 correlated with a synchronous robust decrease in protein level of both total and phosphorylated RB1. Even though the de-phosphorylation of RB1 is not a prerequisite for its further degradation, both transcriptional repression and MDM2-dependent proteasomal degradation are involved in its down-regulation upon CDK4/6 inhibition, which is also an indicator of therapy response. Silencing of MDM2 partially interfered with therapy response in a time-dependent manner. Besides, analysis on the functional and biochemical effects of prolonged CDK4/6 inhibition revealed a partial recovery of cell cycle progression and re-phosphorylation of RB1 under prolonged treatment, accompanied by a precise differential regulation on protein levels of E2F family.

Key words: bladder cancer, target therapy, CDK4/6, RB1, PD-0332991, MDM2

Acknowledgement

Here I would like to thank many people for contributing their efforts to my thesis.This thesis would not have been completed without your help.

First and foremost, I would like to thank my thesis supervisor, Prof. Dr. Gschwend, for providing me the opportunity to do my thesis here.

I wish to express my sincere gratitude to my thesis mentor, PD. Dr. Roman Nawroth. His supervision on me through the years has taught me many lessons on the aspects of scientific research, including experimental design, troubleshooting, scientific writing and critical thinking. He is a very supportive mentor and always approachable for a comprehensive discussion on my work. On the one hand, he kindly offered me some valuable advices on my current concerns and next work. On the other hand, he encouraged me to think critically, raise my own hypotheses and pursue them with his guidance. I am also thankful for the cooperative and relaxed atmosphere of our lab under his leadership.

Thanks also to PD. Dr. Per Sonne Holm for helpful advice and discussions. I am grateful to Dr. Anuja Sathe who started this project and gave me lots of advice and technical support. I would also like to thank Monika Moissl, Klaus Mantwill and Judith Schäfers for their patient assistance on lab routines. I extend my gratitude to all the members of the Nawroth and Holm groups, including Jana Koch, Zhichao Tong, Eva Lichtenegger. The atmosphere in the lab has always been very friendly and cooperative, which made it an excellent place to work.

Many thanks also to China Council Scholar that financially support my study here.

Lastly, I want to thank my family for always supporting me to fulfill my academic goals.

Contents

List of Figures

List of Tables

List of Symbols and Abbreviations

7-AAD	7-aminoactinomycin D
APS	ammonium persulfate
ATM	Ataxia telangiectasia mutated
ATP	Adenosine Triphosphate
ATR	Ataxia Telangiectasia and Rad3 related
BC	bladder cancer
BCA	bicinchoninic acid
BSA	bovine serum albumin
℃	degree Celsius
CaCl2	calcium chloride
CAM	chicken chorioallantoic membrane
CDC6	Cell division control protein 6 homolog
CDK	Cyclin dependent kinases
CDKI	Cyclin dependent kinase inhibitor
cDNA	complementary DNA
CI	combination index
CIP/KIP	CDK interacting protein/Kinase inhibitory protein
CIS	carcinoma in situ
cm	centimeter
CO2	carbon dioxide
CST	Cell Signalling technology
ctrl	control
DDR	DNA damage response
DMEM	Dulbecco's Modified Eagle's Medium
DMSO	dimethylsulfoxide
DNA	deoxyribonucleic acid
DNMT1	DNA methyltransferase 1
DTT	dithiothreitol
EDTA	ethylenediaminetetraacetic acid
EdU	5 ethynyl 2'-deoxyuridine
EGFR	epidermal growth factor receptor
EMT	epithelial-mesenchymal transition

FBS	fetal bovine serum
FDA	Food and drug administration
fmol	femtomole
G1	Gap 1
G2	Gap 2
H2O2	hydrogen peroxide
HCl	hydrogen chloride
HG	high-grade
HPV	human papilloma virus
HRP	horseradish peroxidase
INK4	Inhibitor of CDK4
l	litre
LG	low-grade
m	meter
M	mitosis
MDM2	Mouse double minute 2 homolog
MEK	Mitogen-activated protein **kinase kinase**
mg	milligram
MIBC	muscle invasive bladder cancer
min	minute
ml	millilitre
mM	millimolar
mTOR	the mechanistic target of rapamycin
NaCl	sodium chloride
NaOH	sodium hydroxide
NEAA	non-essential amino acids
ng	nanogram
nm	nanometer
nM	nanomolar
NMIBC	non-muscle invasive bladder cancer
nmol	nanomole
PAGE	polyacrylamide gel electrophoresis
PBS	phosphate buffered saline
PCR	polymerase chain reaction

PD-L1	Programmed death-ligand 1
pH	potentia hydrogenii
PI	phosphatidylinositol
PI3K	phosphatidylinositol-4,5-bisphosphate 3-kinase
PUNLMP	papillary urothelial neoplasm of low malignant potential
PVDF	polyvinylidene fluoride
qPCR	quantitative polymerase chain reaction
RAS	Rat sarcoma
RB	Retinoblastoma
RCF	Relative Centrifugal Force
RNA	ribonucleic acid
RPMI	Roswell Park Memorial Institute
RYBP	RING1 and YY1-binding protein
s	second
S	synthesis
SAHF	senescence-associated heterochromatin foci
SA-β-Gal	senescence-associated β-Gal
SD	standard deviation
SDS	sodium dodecyl sulfate
SE	standard error of the mean
siRNA	small interfering RNA
SRB	sulforhodamine B
TBS	Tris buffered saline
TBST	Tris buffered saline with Tween-20
TCGA	The Cancer Genome Atlas
TEMED	tetramethylethylenediamine
Thr	Threonine
TNM	Tumor, Node, Metastasis
Tris	Tris(hydroxymethyl)-aminomethane
TURBT	transurethral resection of the bladder tumor
V	volt
WT	wild type
YY1	Yin Yang 1
µg	microgram

µl	microlitre
µm	micrometer
µM	micromolar
µmol	micromole

1. Introduction

1.1 Bladder cancer

1.1.1 Epidemiology

Bladder cancer (BC) ranks the eleventh most commonly diagnosed cancer worldwide (Torre et al., 2015). In 2012 the worldwide age-standardized incidence and mortality rates (per 100,000 person/years) are 9.0 and 3.2 for men, respectively. In the female population worldwide, the above two rates are only 2.2 and 0.9 (Torre et al., 2015). The incidence and mortality rates of BC vary across different regions worldwide because of differences in risk factors, methods of diagnosis, and availability of diagnosis and therapy (Burger et al., 2013).

1.1.2 Etiology

The most important risk factor for BC is tobacco smoking, responsible for about 50% of cases (Burger et al., 2013; Chavan, Bray, Lortet-Tieulent, Goodman, & Jemal, 2014). Carcinogens such as aromatic amines and polycyclic aromatic hydrocarbons from tobacco are excreted through urine. Occupational exposure to the above carcinogens is another main risk factor for BC, making up for approximately 10% of all cases. Such occupational exposures take place mainly in industries involved in paint, metal, dye and petroleum products (Burger et al., 2013; Colt et al., 2014). Schistosomiasis, a chronic endemic cystitis due to recurrent infection on bladders with a parasitic trematode, also contributes to most of cases in northern Africa (Burger et al., 2013). Exposure to ionizing radiation is also a risk factor (Burger et al., 2013). Other factors, like family history, fluid intake, hair dye use and dietary habit, seem to have little or uncertain impact on the incidence of BC so far (Burger et al., 2013; Egbers et al., 2015; Vieira et al., 2015). However, genetic predisposition determines susceptibility to other risk factors and therefore influents the incidence of BC. For example, there is a correlation between increased incidence of BC and variation in genes that encodes urea transporters or decarboxylase protein complexes (Cheng, Andrew, Andrews, & Moore, 2016; Garcia-Closas et al., 2011).

1.1.3 Classification of BC

Tumor, node, metastasis (TNM) classification system (Richie et al., 1998) is applied for staging of BC. Histological grading of non-muscle-invasive bladder urothelial carcinomas is performed according to 2004 WHO grading system (Humphrey, Moch, Cubilla, Ulbright, & Reuter, 2016) and consists of three types, papillary urothelial neoplasm of low malignant potential (PUNLMP), low-grade (LG) papillary urothelial carcinoma and high-grade (HG) papillary urothelial carcinoma, according to their potential for invasion and aggressiveness. Papillary tumors invading to the mucosa and the lamina propria are classified as stage Ta and T1, respectively. Flat, high-grade tumors that are confined to the mucosa are classified as CIS (Tis). These tumors are classified as non-muscle invasive bladder cancer (NMIBC), which make up 75-80 % of cases at initial diagnosis (Witjes et al., 2014). The remaining 25% are muscle invasive bladder cancer (MIBC) with classification of stage T2-4 (Fig 1).

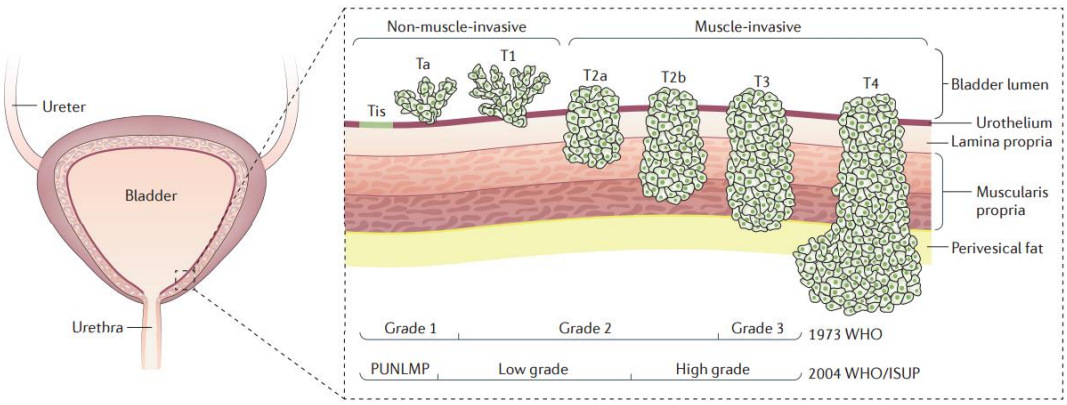

Figure 1: Staging and grading of bladder cancer (Sanli et al., 2017)

1.1.4 Standard therapy for BC

The standard therapy for NMIBC is a combination of transurethral resection of the bladder (TURB) and subsequent intravesical chemotherapy or immunotherapy. Although these patients with NMIBC are expected to have a long-term survival, they face a high risk of five-year recurrence (31-78%) as well as five-year progression to MIBC (1-45%), especially among T1 and Tis (Sathe et al., 2015; Witjes et al., 2014). In fact, the majority of cancer specific deaths are from MIBC. Radical cystectomy combined with necessary pelvic lymph node resection is the standard treatment for MIBC. However, these cases of advanced BC with regional lymph node invasion or

distant metastasis have a quite poor five-year disease specific survival of 14-31%(Sathe et al., 2015). Unfortunately, few therapeutic alternatives with satisfactory therapy response in advanced BC are available, beside cisplatin based chemotherapy regimens. However, it has shown very limited benefits for advanced BC, with a median survival of approximately 14 months. Also, since its approval 30 years ago, it has not been greatly improved or been replaced by other therapies (Witjes et al., 2014), though targeting the immune checkpoint could be a promising therapy in a small ratio of advanced patients (Netto, 2016). Therefore better therapy strategies for advanced BC are urgently required.

1.2 Targeting the CDK4/6-RB1 pathway in BC

1.2.1 The CDK4/6-RB1 pathway regulates G1/S phase transition

A complete cell cycle progression requires transitions of four phases, Gap 1 (G1), synthesis (S), Gap 2 (G2) and mitosis (M), which is sequentially initiated and regulated by a complex of signal pathways. These regulatory pathways are aberrantly activated or inactivated in cancer (U. Asghar, Witkiewicz, Turner, & Knudsen, 2015). As major regulators of cell cycle progression, cyclin dependent kinase (CDK) family, which consists of CDK1, CDK2, CDK4 and CDK6, form complexes with different cyclin proteins, such as cyclin D, E, A and B, and phosphorylate downstream targets of which phosphorylations are required for transitions of respective phases (S. Lim & Kaldis, 2013; Peyressatre, Prevel, Pellerano, & Morris, 2015). Generally the CDKs are constitutively expressed throughout the cell cycle, while their partners, the specific cyclins, are expressed and degraded periodically at restricted phases. As a result, accumulation of specific cyclins and their binding to related CDKs ensure a orderly and timely cell cycle progression (Satyanarayana & Kaldis, 2009). On the other hand, two groups of structural proteins, INK4A inhibitors and CIP/KIP inhibitors, down-regulate activities of CDKs (S. Lim & Kaldis, 2013; Peyressatre et al., 2015).

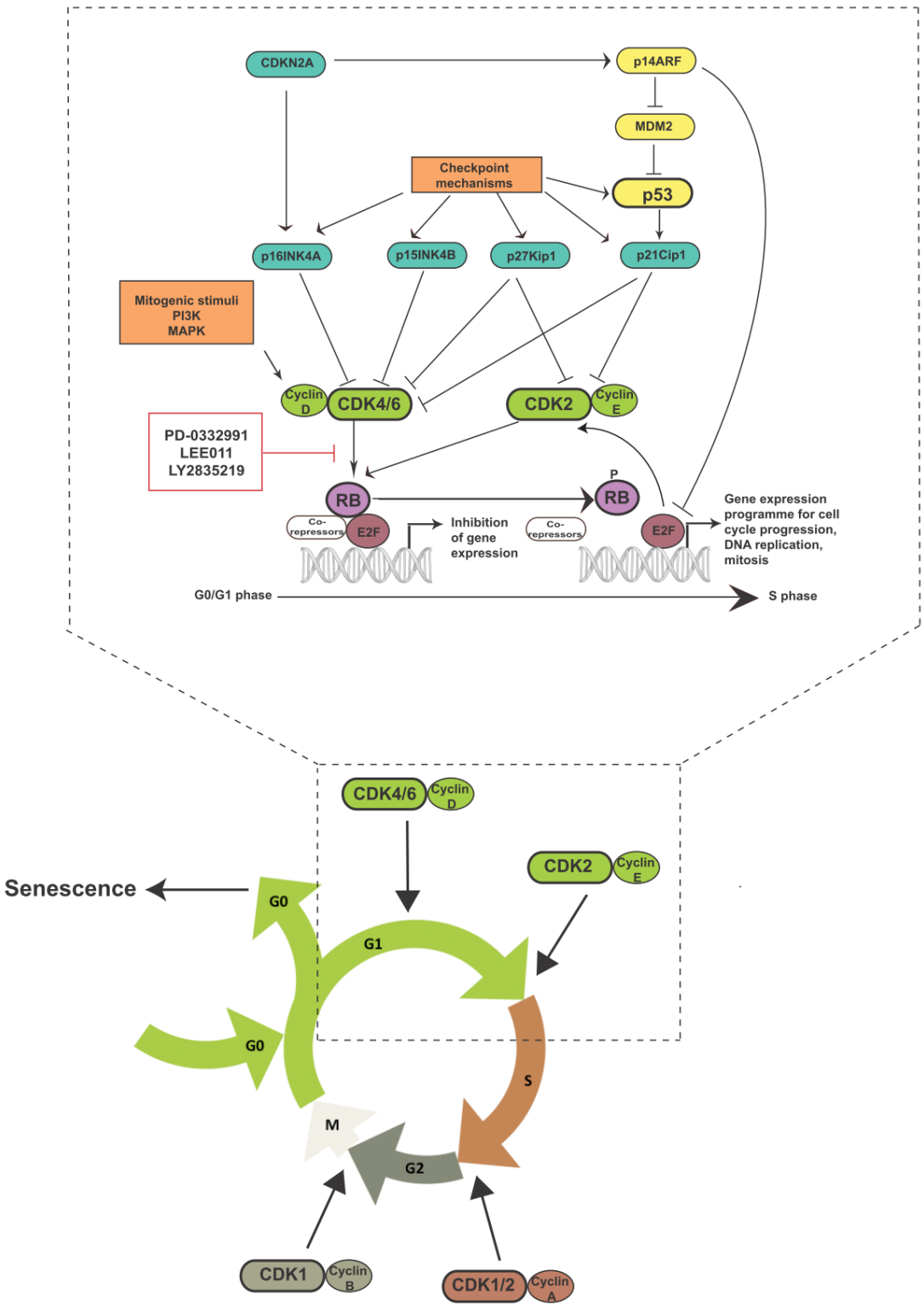

Figure 2: CDK4/6-RB1 pathway (Pan et al., 2017)

RB1 is phosphorylated by complex of CDK4/6 and cyclin D. Phosphorylated RB1 dissociates from transcription factors E2F family, permitting the transcription of E2Fs target genes and cell cycle progression from the G1 to the S phase. Activity of CDK4/6 is also regulated via mitogenic signaling pathways, inhibitor of CDK4 (INK4)

and p53 dependent checkpoint. Small molecule inhibitors of CDK4/6 inhibit phosphorylation of RB1 and transition from G1 to S phase.

The transition of cell cycle from G1 phase into S phase is initiated by the activation of CDK4 and CDK6 of which structures and functions are highly homologous. The activation of CDK4/6 requires the formation of a complex with their partners cyclin D proteins. Cyclin D proteins that are made up of three subtypes, cyclin D1-3, can accumulate immediately upon mitogenic stimuli (U. Asghar et al., 2015) (S. Lim & Kaldis, 2013; Satyanarayana & Kaldis, 2009). Inhibitor of CDK4 (INK4) family, including p16INK4A, p15INK4B, p18INK4C and p19INK4D, are negative regulators of CDK4/6. They interact with CDK4/6 and inhibit their activity, either by reducing their binding with cyclin D1 or by directly occupying their catalytic domains (Sherr & Roberts, 1999).

The active CDK4/6-cyclin D1 complex induces the phosphorylations of the retinoblastoma (RB) protein family including RB1, p107 and p130 (U. Asghar et al., 2015; Giacinti & Giordano, 2006; Peyressatre et al., 2015). The function of RB1 relies on its phosphorylation status. In quiescent cells, hypophosphorylated RB1 of high activity combines tightly to transcriptional factor E2F family members (E2Fs), with recruitment and assembly of other co-repressors, and suppresses the transcriptional activity of E2Fs. However, upon the phosphorylating from CDK4/6, the inactive phosphorylated RB1 detaches from E2Fs and initiates the transcription of their target genes required for the transition of cell cycle into S stage, including cyclin A, cyclin E, CDK2, DHFR (dihydrofolate reductase), MCM (minichromosome maintenance) family (Giacinti & Giordano, 2006). Therefore, inhibition of CDK4/6 represses the phosphorylation of RB1 and transcriptional activity of E2Fs, theoretically preventing the cell cycle progression into S phase (Fig 2).

Beside the CDK4/6-RB1 pathway, cell cycle checkpoint dominated by p53 is also playing a role in arresting cell cycle before S phase. Cell cycle checkpoints are surveillance mechanisms that ensure the genomes to be passed accurately to the next generation. When genotoxic stresses cause DNA damages, the checkpoints are able to detect them and further arrest the cell cycle to allow time for repairing the damaged DNA before they are passed to the daughter cells (Abraham, 2001). Upon

DNA damage, the activation of p53 is due to its improved stability, which is attributed to the phosphorylation directly or indirectly by kinase ATM (Ataxia telangiectasia mutated) or ATR (Ataxia Telangiectasia and Rad3 related), a pair of DNA damage sensors. Mouse double minute 2 homolog (MDM2) is an important negative regulator of p53. As an ubiquitin ligase, it causes the ubiquitination and subsequent degradation of p53 via proteasome. Thus, increased levels or aberrantly activation of MDM2, which are common in cancer, would inactivate the tumor suppressive function of p53, such as apoptotic induction and cell cycle arrest. On the other hand, the phosphorylation on p53 interrupts the interaction between MDM2 and p53, and thereby prevents p53 from being degraded (Abraham, 2001; Moll & Petrenko, 2003). The accumulation of p53, as a transcriptional activator, increases the transcription of cyclin dependent kinases inhibitor, p21 (Kip1) (el-Deiry et al., 1993). P21 suppresses the activity of CDK2 and thereby prevents the cell cycle progression into S phase (Sherr & Roberts, 1999). P14 (ARF) is also encoded by gene INK4A and functions as a cell cycle negative regulator. However, unlike p16 that is involved in the CDK4/6-RB1 pathway, p14 arrests G1/S phase in a p53 dependent manner. It binds to MDM2 and induces a rapid degradation of MDM2, resulting in concurrent the stabilization and accumulation of p53 (Pomerantz et al., 1998). Besides p53 and p14, some additional MDM2 interacting partners have been identified. For instance, MDM2 also interacts with RB1 through its C-pocket domain and suppresses RB1 function by interfering with formation of the RB1-E2F-DNA complex, which indicates a crosstalk between the RB1-dependent and p53-dependent pathway in regulating G1/S transition. Thus, more functions of MDM2 independent of p53 remained further identified.

1.2.2 Disruption of the CDK4/6-RB1 Pathway in Cancer results in uncontrolled cell growth

Cell cycle deregulation is a common feature of cancer cells that leads to uncontrolled cell proliferation. This includes the disruption of the CDK4/6-RB1 signaling pathway and an uncontrolled G1/S transition of the cell cycle. One of the common mechanisms is inactivation of RB1 through molecular alterations such as loss of function mutations or deletions. RB1 was the first tumor suppressor identified and its inactivation is considered to be a hallmark feature of retinoblastoma and small cell lung cancer (Knudsen & Knudsen, 2008). Some viral oncoproteins, such as the E7

from the human papilloma virus (HPV), can also directly bind to RB1 and release E2F from the RB1-E2F complex. This interaction between E7 and RB1 acts as another style of RB1 inactivation, which is mainly observed in HPV associated cancers such as cervical carcinoma (Knudsen & Knudsen, 2008; Munger et al., 2001).

The CDKN2A gene locus encodes for the CDK4/6 inhibitor proteins p15INK4B and p16INK4A, as well as the tumor suppressor p14ARF. Copy number loss, loss of function mutations as well as epigenetic silencing of p16INK4A is commonly observed in several tumor entities (Liggett & Sidransky, 1998; Witkiewicz, Knudsen, Dicker, & Knudsen, 2011). p16INK4A loss is also frequently observed in premalignant lesions, suggesting that it is an initial mechanism to enable cellular transformation (Liggett & Sidransky, 1998). Some tumors and premalignant lesions also demonstrate an elevated expression of p16INK4A that is often mutually exclusive with loss of RB1 function, suggesting that it is a mechanism to compensate for the cell cycle deregulation induced by RB1 loss (U. Asghar et al., 2015; Collado et al., 2005; LaPak & Burd, 2014; Liggett & Sidransky, 1998; Witkiewicz et al., 2011). On the contrary, elevated p16INK4A expression in the presence of functional RB1 is observed in some premalignant lesions, which might reflect a protective response to oncogene induced senescence and DNA damage in order to limit cell proliferation (Collado et al., 2005; Liggett & Sidransky, 1998; Serrano, Lin, McCurrach, Beach, & Lowe, 1997).

The amplification and overexpression of cyclin D1 are frequently observed in breast cancer, esophageal, lung, liver, bladder cancer and so on, but both have no correlation to each other and can exist independently (Buckley et al., 1993; Jiang et al., 1992; Tashiro, Tsuchiya, & Imoto, 2007). Cyclin D1 nuclear export initiates once its Thr-286 residue is phosphorylated. However, in primary esophageal carcinoma samples the mutation of Thr-286 widely existed, which convert this residue into a non-phosphorylatable one. The unphosphorylated cyclin D1 constitutively locates in the nuclei and add its oncogenetic potential (Benzeno et al., 2006). In addition, the amplification of CDK4 has been mainly reported in sarcomas (Khatib et al., 1993; Park et al., 2014).

1.2.3 Target therapy in bladder cancer

From 1990s, target therapy was introduced to cancer treatment. The principle of these therapies is to block the cellular molecular pathway that is necessary for cancer viability and development. A growing number of targeted therapies have been approved by FDA for cancer therapy, such as Trastuzumab for HER2 positive breast cancer and Imatinib for Philadelphia chromosome positive leukemia.

Programmed death ligand 1 (PD-L1) antibody that targets the immune checkpoint was granted food and drug administration (FDA) approval for treating metastatic BC (Netto, 2016). According to an initial study, this antibody was only efficacious in tumors that express PD-L1, which represented only 27% of patients in this cohort. Hence, despite promising results from immunotherapy, other novel treatment strategies are still required to target a higher proportion of BC.

Unfortunately, beside PD-L1 antibody, until now no other target therapy has been approved by FDA or performed in phase III for BC treatment, though more and more target therapies whose efficiency have been validated in other cancers are being studied in all stages of clinical trials for BC (Ghosh, Brancato, Agarwal, & Apolo, 2014). The majority of trials where specific inhibitors were used to activate or inactivate certain cell signaling pathways have demonstrated limited efficiency (Ghosh et al., 2014). Most of these trials were conducted without including pre-stratification of patients based on specific biomarkers. For example, in non-small-lung cancer, the therapeutic effectiveness of Gefitinib, an epidermal growth factor receptor (EGFR) inhibitor, depends on the existence of EGFR mutation (Mok et al., 2009). Given the molecular heterogeneity existed in BC, this might be a major drawback in their trial design (Carneiro et al., 2015).

1.2.4 CDK4/6 is a potential therapeutic target in bladder cancer

A better understanding of molecular biology in these aggressive BCs will help to identify novel target therapies. The Cancer Genome Atlas (TCGA) has recently published a more comprehensive insight into the genetic landscape of invasive BC. MIBCs were classified as different subtypes or clusters based on their genetic backgrounds. Individualized target therapies might be developed for these subtypes.

Whole-exome sequencing of 131 invasive BC samples were analyzed for their somatic mutation and DNA copy-number data. Three main pathways involved in cell cycle regulation, chromatin remodeling and kinase signaling were identified dysregulated frequently in BC (Taylor et al., 2014). Genetic alterations involved cell cycle regulation, such as RB1, CDKN2A, P53 and CCND1 were existed in 93% of invasive BC (Taylor et al., 2014). These alterations may indicate a disruption of balanced cell cycle regulatory mechanism in BC and thus provide a biological rational for therapeutic targeting. CDK4/6-RB1 pathway is a leading pathway that regulates the progression of cell cycle from G1 phase to S phase, and can be targeted by selective CDK4/6 inhibitor. Inspiringly, CDK4/6 inhibition, as a combinatory therapy with endocrine therapy, has been approved to improve the survival in women with hormone receptor-positive metastatic breast cancer, and is therefore approved by FDA for breast cancer therapy (Cristofanilli et al., 2016; Hortobagyi et al., 2016). We have discussed current pre-clinical and clinical developments of CDK4/6 inhibitors in cancer therapy, their potential application in BC therapy and the challenges to be solved in a published review (Pan et al., 2017).

1.2.5 Targeting the CDK4/6-RB1 pathway in cancer

Several ATP-competitive small molecules have been developed in order to inhibit the catalytic function of CDKs (U. Asghar et al., 2015; Dickson, 2014; Peyressatre et al., 2015). However, first generation inhibitors such as Favopiridol are non-selective and can inhibit CDK1, CDK2, CDK4, CDK6, CDK7 and CDK9 (Dickson, 2014). This non-specificity might be responsible for the limited efficacy and high toxicity in clinical trials (U. Asghar et al., 2015; Peyressatre et al., 2015). Next generation CDK4/6 inhibitors are highly selective and include PD-0332991 (Pfizer) (Fry et al., 2004), LY-2835219 (Eli Lilly) (Tate et al., 2014) and LEE011 (Novartis) (Rader et al., 2013). All these inhibitors are proposed to inhibit CDK4/6 activity at nanomolar concentrations, and are highly specific.

These CDK4/6 inhibitors have been tested pre-clinically in in vitro and in vivo models of hematological cancers (Divakar et al., 2015; Marzec et al., 2006; Sawai et al., 2012; L. Wang et al., 2007) and solid tumors including breast cancer (Dean et al., 2012; Dean, Thangavel, McClendon, Reed, & Knudsen, 2010; Finn et al., 2009; Kovatcheva et al., 2015; Vora et al., 2014; Witkiewicz, Cox, & Knudsen, 2014),

melanoma (Mahgoub et al., 2015; Menu et al., 2008; Yadav et al., 2014; Young et al., 2014), glioma (Barton et al., 2013; Michaud et al., 2010; Wiedemeyer et al., 2010), pancreatic cancer (Franco, Witkiewicz, & Knudsen, 2014; Heilmann et al., 2014; F. Liu & Korc, 2012; Witkiewicz et al., 2015), hepatocellular carcinoma(Rivadeneira et al., 2010), lung adenocarcinoma(Fry et al., 2004; Puyol et al., 2010), sarcoma(Kennedy et al., 2015; Kovatcheva et al., 2015; Olanich et al., 2015; Perez, Munoz-Galvan, Jimenez-Garcia, Marin, & Carnero, 2015a; von Witzleben et al., 2015; Zhang et al., 2014), ovarian cancer (Konecny et al., 2011), renal cancer(Logan et al., 2013), prostate cancer (Comstock et al., 2013), bladder cancer (Sathe et al., 2015), neuroblastoma (Rader et al., 2013) and chordoma (von Witzleben et al., 2015). Most studies showed, upon CDK4/6 inhibition, a consistent molecular and functional phenotype that a reduction in expression of total and phosphorylated RB1 as well as transcription of E2Fs target genes correlated with a G0/G1 arrest and cytostatic effect. In addition, all these studies demonstrated that presence of RB1 is a pre-requisite for therapy response and RB1 negative cells are non-responsive.

Our group evaluated the potential of CDK4/6 inhibition as a target therapy in BC. The effect of PD-0332991 was tested on 10 BC cell lines and a three-dimensional tumor xenograft model using the chicken chorioallantoic membrane (CAM) (Sathe et al., 2015). Only RB1 positive BC cell lines are responsive to the treatment of PD-0332991, with the cell cycle being arrested in G1 phase. We also observed a synchronous reduction in both total and phosphorylated RB1 upon treatment. This decrease in total RB1 was partially due to a reduction in its transcription. These results suggest that CDK4/6 inhibition has the potential to be an effective therapeutic strategy in BC. However, several areas need further investigation in order to enable an effective transition from experimental models to clinical success.

1.2.6 Molecular mechanism of CDK4/6 inhibition

The mechanism how CDK4/6 inhibition regulates cancer growth is via an induction of G0/G1 cell cycle arrest. This is achieved by blocking kinase activity of CDK4/6 on RB1. Decreased level of phosphorylated RB1 upon CDK4/6 inhibition has been observed consistently in many pre-clinical studies. However, in most studies including leukemia, breast cancer, myeloma, glioma, pancreatic cancer, ovarian cancer, bladder cancer and chordoma (Barton et al., 2013; Dean et al., 2010; Finn et

al., 2009; Franco et al., 2014; Konecny et al., 2011; F. Liu & Korc, 2012; Menu et al., 2008; Miller et al., 2011; Sathe et al., 2015; Sawai et al., 2012; von Witzleben et al., 2015; Witkiewicz et al., 2015), this is also accompanied by a synchronous reduction in total RB1 protein level. Though the status of RB1 is a key determinant of therapy response to CDK4/6 inhibitors, this observation on reduction of total RB1 and its possible mechanism behind have been neither described nor discussed clearly. This implies that a better understanding of total and/or phosphorylated RB1 protein level in CDK4/6 inhibition will contribute to a better understanding of genetic determinants that are crucial for therapy response. Our group has shown a downregulation of RB1 transcription upon CDK4/6 inhibition (Sathe et al., 2015). It was reported RB1 and other RB family members (p107 and 130) auto-regulate their transcription (Burkhart et al., 2010; Gill et al., 1994; Hamel, Gill, Phillips, & Gallie, 1992). In vitro and in vivo, RB1 gene product p110 is able to bind to the promoter of RB1 and suppress its transcription, while loss of RB1 generally increases its own transcription (Burkhart et al., 2010; Gill et al., 1994; Hamel et al., 1992). Compared to p110, p130 can positively regulation RB1 promoter activity (Burkhart et al., 2010). However, depending on cell specific context, p110 may either negatively or positively regulate its own promoter (Burkhart et al., 2010).

We then addressed whether RB1 protein is degraded via proteasome upon CDK4/6 inhibition. The addition of MG-132, a proteasome inhibitor, did not prevent RB1 degradation upon CDK4/6 inhibition, indicating that the reduction of RB1 was not predominantly via proteasome-dependent degradation. However, another recent study showed a rescue of RB1 degradation using a high concentration of MG-132 (1uM) in melanoma (Yoshida, Lee, & Diehl, 2016). MG-132, as a non-specific proteasome inhibitor, has high cytotoxicity. So a much lower concentration of MG-132 (100 nM) was applied in our model since it did not exhibit robust cytotoxicity in cell viability assays but should be enough to inhibit proteasome activity according to the literature (Tsubuki, Saito, Tomioka, Ito, & Kawashima, 1996). The very different concentration of MG-132 used in the two studies can account for the contradictory observations on rescue of RB1 reduction. Therefore, further studies introducing more specific proteasome inhibitors and other methods to manipulate this pathway is required to validate this inconsistency.

1.2.7 Functional effects of CDK4/6 inhibition

All published reports have demonstrated that CDK4/6 inhibitors are capable of arresting cells in the G0/G1 phase. Hence it is important to investigate whether the cell cycle arrest induced by CDK4/6 inhibition, when the inhibitors are removed, is reversible or permanent. The permanent and irreversible cell cycle arrest was first described and defined as senescence by Hayflick in 1965 (Hayflick & Koprowski, 1965). Senescent cells are detected by the presence of several molecular markers and features including a large morphology, growth arrest, senescence-associated β-Gal (SA-β-Gal) staining, senescence-associated heterochromatin foci (SAHF), and markers of the DNA damage response (DDR) (Bernardes de Jesus & Blasco, 2012) (Campisi & d'Adda di Fagagna, 2007; Collado & Serrano, 2010; Kuilman, Michaloglou, Mooi, & Peeper, 2010).

It has been reported that prolonged CDK4/6 inhibition (>3 days) induced senescence in a subpopulation of cancer cells in vitro and in vivo (Heilmann et al., 2014; Kovatcheva et al., 2015; Michaud et al., 2010; Wiedemeyer et al., 2010) (Acevedo et al., 2016a; Perez, Munoz-Galvan, Jimenez-Garcia, Marin, & Carnero, 2015b; Yoshida et al., 2016) (Bourdeau & Ferbeyre, 2016). However, since the induction of senescence is insufficient, the remaining senescence-resistant subclones are able to restore cell cycle progression upon the removal of CDK4/6 inhibition. The latest studies in vivo demonstrating that chronic CDK4/6 inhibition failed to maintain a persisting cell cycle arrest on tumor cells even after the initial stable disease also support the observation (Herrera-Abreu et al., 2016; Yoshida et al., 2016). Although CDK4/6 inhibition merely induced a partial senescence in the examined tumors, the resistance to senescence existed in other subclones probably is due to activation of other oncogenic pathways and might be overcome by additional specific inhibitors. For instance, extended CDK4/6 inhibition induce 80% of melanoma cells to undergo senescence, while the remaining proportion escape senescence because of a re-activation of mTORC1 pathway via induction of Raptor. Both Raptor knockdown and mTOR inhibitor rapamycin can overcome its resistance to senescence(Yoshida et al., 2016). The latest studies also reveal a CDK4/6 dependent epigenetic pathway through which cancer cells can escape a complete senescence. And the CDK4/6 inhibition can re-sensitize the cells to induction of senescence through an autophagy

dependent degradation of DNMT1 (DNA methyltransferase 1) (Acevedo et al., 2016b; Bourdeau & Ferbeyre, 2016).

Early adaption, not resistance, to CDK4/6 inhibition was also observed in leukemia, breast cancer and liposarcoma cells (Herrera-Abreu et al., 2016; Zhang et al., 2014) (L. Wang et al., 2007). Under prolonged CDK4/6 inhibition for 48 hours or longer, these sensitive cells of functional RB1 underwent a partial recovery of cell cycle progression, compared to those upon 24 hours of treatment. The adaption to prolonged CDK4/6 inhibition has been demonstrated to be supported by a compensative activation of CDK2 pathway, probably due to increased adaptive PI3K signaling (Herrera-Abreu et al., 2016) or down-regulation of p27 (Kip) (L. Wang et al., 2007). In addition, cancer cells acquired a loss of RB1 to evolve into resistant clones during long term treatment (Herrera-Abreu et al., 2016). Therefore, if these inhibitors are only able to function maximally during a very short time window (24 hours), a 3 week on / 1 week off regime used for CDK4/6 inhibitors in the clinic might not be ideal for tumor suppression. Novel combination or sequential therapy strategies are required for improved efficiency.

Interestingly, other effects induced by CDK4/6 inhibition such as apoptosis and epithelial-mesenchymal transition (EMT) have been also reported in some carcinomas (Barton et al., 2013; Konecny et al., 2011; F. Liu & Korc, 2012; Sawai et al., 2012; Yadav et al., 2014), but few explanation was addressed to these effects. LY2835219 induced robust apoptosis in tumor deprived vemurafenib-resistant melanoma cells, while no apoptosis was observed in the parental vemurafenib-sensitive cells (Yadav et al., 2014). Also, prolonged treatment with PD-0332991 for 5 days induced a modest apoptosis among ovarian cancer cell lines (Konecny et al., 2011). EMT induced by CDK4/6 inhibition fueled the invasion of SMAD-4 wild-type pancreatic cancer cell through activating TGF-β pathway (F. Liu & Korc, 2012). Further studies are required for evaluating these phenotypes to reveal their implications in therapy response to CDK4/6 inhibitors.

1.2.8 Biomarkers for personalizing CDK4/6 target therapy

The therapy response to CDK4/6 inhibition is likely to be regulated via a complex of molecular mechanisms. A comprehensive Identification of these underlying

mechanisms contributes to a development of potential biomarkers that can be applied for pre-stratification of patients who will benefit from the therapy, based on the genetic landscape of their tumors. Pre-clinical studies have consistently suggested mainly based correlation studies in RB1 positive and negative cell lines that RB1 expression is a pre-requisite for sensitivity to CDK4/6 inhibition (Comstock et al., 2013; Fry et al., 2004; Konecny et al., 2011; Michaud et al., 2010; Sathe et al., 2015; von Witzleben et al., 2015; Young et al., 2014) and that primary sensitive cells with an acquired loss of RB1 develop into resistant cells (Herrera-Abreu et al., 2016; Witkiewicz et al., 2015).

However, few studies that attempted to confirm the role of RB1 in therapy response by manipulating RB1 expression in cells have contradictory findings. We have demonstrated that introduction of recombinant RB1 protein in RB1 negative BC cells fails to re-sensitize them to CDK4/6 inhibitors (Sathe et al., 2015). Similar confusion has been also observed that reconstitution of exogenous RB1 in RB1 negative breast cancer and retinoblastoma cell lines was unable to reverse their malignant phenotypes(Muncaster, Cohen, Phillips, & Gallie, 1992). On the other hand, although RB1 positive liposarcoma cells turned resistant to CDK4/6 inhibition after siRNA mediated silencing of RB1 expression (Zhang et al., 2014), similar effect was not observed in RB1 positive breast cancer and hepatoma cells (Dean et al., 2010; Rivadeneira et al., 2010). These seemingly contradictory findings might be explained by different mechanisms for regulating cell cycle progress between RB1 positive and negative cells. For example, RB1 deficient cells rely on alternative mechanism to regulate the G1/S transition, which is independent of the CDK4/6-RB1 pathway (H. Liu et al., 2015). Hence, reconstitution of RB1 in these cells failed to convert the regulatory mechanism for G1/S transition to a RB1 dependent way, so that CDK4/6 inhibition has no effect on cell cycle progression. Conversely, acute silencing expression of RB1 with siRNA in RB1 positive cells failed to mimic the identical disrupted molecular pathways that are existed in intrinsic RB1 negative cells. Moreover, this acute loss of RB1 is compensated by other RB family members such as p107 and p130 (Dean et al., 2010; Rivadeneira et al., 2010). These potential mechanisms make it quite challenging to directly evaluate the role of RB1 expression in the therapy response to CDK4/6 inhibition.

In addition to RB1, loss of p16INK4A, overexpression of cyclin D1 and amplification of CDK4 correlated with sensitivity to CDK4/6 inhibitors in different models (Barton et al., 2013; Finn et al., 2009; Konecny et al., 2011; Puyol et al., 2010; von Witzleben et al., 2015; Wiedemeyer et al., 2010; Young et al., 2014). Increased expression of E2F2 renders breast cancer and hepatoma resistance to CDK4/6 inhibition (Dean et al., 2010; Rivadeneira et al., 2010). Compensatory activation of the CDK2 pathway via up-regulation of cyclin D1, E or A and down-regulation of p21 and p27 has also been demonstrated to contribute to therapy resistance (Dean et al., 2010; Franco et al., 2014; Herrera-Abreu et al., 2016; L. Wang et al., 2007). Reduced level of MDM2 improved therapy response to PD-0332991 via a more thorough induction of senescence (Kovatcheva et al., 2015). Ectopic activation of mitogenic pathways, like mTOR and MEK pathways, was observed in breast and pancreatic cancer with acquired resistance to CDK4/6 inhibition (Franco, Balaji, Freinkman, Witkiewicz, & Knudsen, 2016; Knudsen & Witkiewicz, 2016).

Preliminary correlation analyses from tumors treated with CDK4/6 inhibitors in clinical trials also demonstrated potential biomarkers. In advanced breast cancer, estrogen receptor (ER) positive and HER2 negative expression status was significantly associated with response to PD-0332991 in combination with hormone therapy. However, additional biomarkers such as amplification of CCND1 or loss of CDKN2A were not predictive of therapy response (DeMichele et al., 2015; Finn et al., 2015). Abemaciclib mono-therapy was also recently tested in a variety of solid tumors (Patnaik et al., 2016). In this trial, responses were also observed in HER2 negative breast cancer, with no clear correlation to CDKN2A, CDKN2B, CCDN1, RB1, CCNE1, PIK3CA or PTEN status. In a trial examining ribociclib monotherapy in a variety of solid tumors, CCDN1 amplified and CDKN2A/CDKN2B co-deleted tumors had a trend towards a longer duration of treatment response. However, no clear correlation emerged between therapy response and molecular alterations in RB1, CDKN2A, CDKN2B and CCND1 (Infante et al., 2016). Hence, the present evidence suggests that there are distinct subsets of patients that respond to CDK4/6 inhibitors. However, until now the ER positive / HER2 negative breast cancer is the only clinically reliable biomarker to predict the response to CDK4/6 inhibition. Other markers which are potential in preclinical trials have never been confirmed in patients. Investigations

relying on genomic analyses of tumor tissues from patients can promisingly fuel the development of a personalized target therapy strategy.

1.2.9 Combination therapy with CDK4/6 inhibitors

Combination therapy of CDK4/6 inhibitors with other agents has the potential to improve efficacy or to overcome resistance. This strategy can be used to improve responses seen with standard chemotherapy regimens. However, various chemotherapy agents are effective only in specific cell cycle stages (Valeriote & van Putten, 1975). This can lead to either antagonistic, additive or synergistic effects in combination with CDK4/6 inhibitors. Such effects are quite complicated and can be tumor type, chemotherapy option and therapy sequence dependent. We have observed that combination of PD-0332991 and cisplatin have a synergistic effect on BC cells (Sathe et al., 2015), but an antagonistic effect on pancreatic ductal adenocarcinoma cell (Franco et al., 2014). Additive or synergistic interactions were observed when a combinative CDK4/6 inhibition was given concomitantly with carboplatin or paclitaxel in ovarian cancer cells, while 24 hours of CDK4/6 inhibition before the following chemotherapy caused a antagonistic effect (Konecny et al., 2011). In most pancreatic ductal adenocarcinoma cell lines, CDK4/6 inhibition weakened gemcitabine-mediated toxicity but increased the cytotoxicity of 5-FU (Franco et al., 2014).

CDK4/6 inhibitors have also been combined with different target therapies. A synergistic effect was observed with a combination of PD-0332991 and endocrine therapy in ER positive and HER2-amplified breast cancer cell lines (Finn et al., 2009). The combination therapy not only cooperate for the inhibition of cell cycle progression and block compensatory mitogenic pathways that could contribute to therapeutic resistance (Herrera-Abreu et al., 2016; Knudsen & Witkiewicz, 2016) but also increase the responsiveness to ER antagonism (Yang et al., 2016). Consistently, this was also reflected in clinical trials where patients receiving a combination of hormone therapy and PD-0332991 had better survival as compared to those receiving single hormone therapy (Cristofanilli et al., 2016; Hortobagyi et al., 2016). It has been demonstrated that increased activity in PI3K-mTOR pathway contributes to the resistance to CDK4/6 inhibitors (Franco et al., 2016; Heilmann et al., 2014; Yoshida et al., 2016). As a result, p16INK4A deficient pancreatic ductal

adenocarcinoma (PDAC) cells were sensitized to CDK4/6 inhibition by using an mTOR inhibitor (Heilmann et al., 2014). Also, melanoma cells escaped senescence under prolonged CDK4/6 inhibition via re-activation of mTORC1 pathway, and mTOR inhibitor rapamycin can prevent its resistance to senescence (Yoshida et al., 2016). In KRAS mutant colorectal cancers and non-small cell lung cancer cells as well as neuroblastoma with hyperactivated RAS-MAPK signaling, a combination of CDK4/6 inhibitor and MEK inhibitor has been proved more effective pre-clinically (Lee et al., 2016; Tao et al., 2016) (Hart et al., 2016).

1.3 Outlook

CDK4/6 inhibitors have demonstrated efficiency in various tumor entities in pre-clinical and clinical studies, with an established safety profile. The FDA has recently granted breakthrough therapy approval for all three CDK4/6 inhibitors in the treatment of HER2 negative, hormone receptor positive metastatic breast cancer (Cristofanilli et al., 2016; Hortobagyi et al., 2016; Sledge et al., 2017). We have demonstrated that CDK4/6 inhibition is a promising strategy in BC to limit cellular proliferation and tumor growth, which is being further tested clinically. The combination of PD-0332991 and cisplatin is being investigated in a phase I clinical trial for patients with unresectable BC (NCT02897375). Meanwhile, amplification of CDK4/6 or cyclinD1-3 and presence of RB1 are being tested for potential biomarkers predicting therapy response in a phase II clinical trial (NCT02465060). Although CDK4/6 is a promising target in BC, further research is required to improve its delivery in clinic. This includes a thorough understanding of the molecular mechanisms that mediate the response to CDK4/6 inhibition. Another major area that requires investigation is the identification of biomarkers of response and resistance to these inhibitors, which will aid in the development of personalized therapy. More efforts should also be focused on determining effective treatment schedules as well as potential combination therapy strategy that so as to improve therapy efficiency and minimize the acquisition of resistance.

1.4 Aims and objectives of this project

Since the CDK4/6-RB1-E2F pathway is one of the most frequently altered signal pathways in advanced BC according to TCGA, we have evaluated the potential of this target therapy using a CDK4/6 inhibitor, PD-0332991, in the therapy for BC pre-

clinically. We observed that all therapy responsive BC cell lines are RB1 positive. Also, apart from the phosphorylation of RB1, its total protein level is also decreased among these responsive cell lines upon CDK4/6 inhibition, which is poorly studied and interpreted. In the current completed phase III clinical trials, there is no evidence that the presence of RB1 is a reliable biomarker to predict therapy response to CDK4/6 inhibitors, which also indicates a high complexity of molecular mechanisms underlying CDK4/6 inhibition. So a more thorough understanding of the regulatory network induced by CDK4/6 inhibition is urgently required for optimizing its therapeutic strategy. In this project, we aimed to:

a) Characterize molecular mechanisms induced by CDK4/6 inhibition
b) Analyze the effects of these molecules on therapy response
c) Characterize the implication of RB1 expression and degradation in therapy response
d) Analyze the therapy response to prolonged CDK4/6 inhibition

2. Materials

2.1 Equipments and machines

Equipments and machines	Manufacturer
Autoclave Sytec DX-65	Systec GmbH, Linden, Germany
Biological safety cabinet Herasafe KS12	Thermo Scientific, Waltham, MA, USA
Analytical balance AT250	Mettler Toledo, Gießen, Germany
Analytical balance Sartorius 2254	Sartorius, Göttingen, Germany
Automatic film processor Curix CP1000	Agfa Healthcare, Mortsel, Belgium
BD FACSCalibur Flow Cytometry System	BD Biosciences, San Jose, CA, USA
BVC professional laboratory fluid aspirator	Vacuubrand Gmbh, Wertheim, Germany
Centrifuge ROTINA 35R	Hettich, Tuttlingen, Germany
Centrifuge 5810R	Eppendorf GmbH, Hamburg, Germany
Chemidoc™ XRS Imaging System	BioRad, Hercules, CA, USA
Cryogenic Freezing Container, 1 Deg C	Nalgene, Rochester, NY, USA
CO2 incubator HERA Cell240	Thermo Scientific, Waltham, MA, USA
Electrophoresis Power Supply EPS 601	Amersham Pharmacia Biotech., Uppsala, Schweden
Heating and drying oven Heraeus FunctionLine B6	Thermo Scientific, Waltham, MA, USA
Heating block thermostat BT100	Kleinfeld Labortechnik, Gehrden, Germany
Ice machine Manitowoc	Manitowoc Ice, Manitowoc, WI, USA
Intellimixer RM-2L	Elmi Ltd. Laboratory Equipment, Calabasas, CA, USA
Magnetic Stirrer	Heidolph Instruments GmbH, Schwabach, Germany

Microcentrifuge 5430R	Eppendorf GmbH, Hamburg, Germany
Mini-PROTEAN Tetra Cell gel system	BioRad, Hercules, CA, USA
Mini Trans-blot cell transfer system	BioRad, Hercules, CA, USA
Mini Protean System	BioRad, Hercules, CA, USA
Minishaker IKA® MS2	IKA Works Inc., Staufen, Germany
Multilabel plate reader VICTOR™ X3	Perkin Elmer, Waltham, MA, USA
Microplate reader Vmax Kinetic	Molecular Devices, Sunnyvale, CA, USA
Microscope camera AxioCam ERc 5s	Carl Zeiss, Oberkochen, Germany
Microscope AxioVert.135	Carl Zeiss, Oberkochen, Germany
Microscope AxioVert.A1	Carl Zeiss, Oberkochen, Germany
Micropipettes PIPETMAN P2, 10, 20, 200, 1000	BD Biosciences, San Jose, CA, USA
Neubauer chamber	LO Laboroptik, Lancing, England
Orbital shaker K15	Edmund Bühler GmbH, Hechingen, Germany
pH Meter 691	Metrohm, Filderstadt, Germany
Power supply PowerPac HC	BioRad, Hercules, CA, USA
PerfectBlue Gelsystem Mini M	PEQLAB Biotechnologie GmbH, Erlangen, Germany
Spectrophotometer Nanodrop 2000c	Thermo Scientific, Waltham, MA, USA
Thermal cycler C1000™ CFX96™	Bio-Rad, Hercules, CA, USA
Thermal cycler iCycler iQ ™ Real-time PCR detection system	BioRad, Hercules, CA, USA
Thermal cycler MJ Research PTC-200	BioRad, Hercules, CA, USA
Vortex-Genie® 2	Scientific Industries, Inc., Bohemia, NY, USA
Water bath W350	Memmert, Schwabach, Germany

Table 1: Equipments and machines

2.2 Disposable equipments

Disposable equipments	**Source**
Amersham hybond-P PVDF-Membrane	GE-Healthcare, Buckinghamshire,

	England
Cell culture plates 96 well, 24 well, 12 well, 6 well, 10 cm	Coming Incoporated, Coming, NY, USA
Chromatography paper Whatman	GE Healthcare, Buckinghamshire, England
Conical bottom polystyrene tubes	Elkay, Hampshire, United Kingdom
Conical tubes 15ml, 50ml Falcon	Greiner GmbH, Frickenhausen, Germany
Cryogenic vials 1.8 ml Nunc	Sigma-Aldrich Chemie GmbH, Munich, Germany
Hard-Shell PCR Plates 96-well	BioRad, Hercules, CA, USA
Lens cleaning paper	The Tiffen company, Hauppauge, NY, USA
Microscope coverslips	Thermo Scientific Waltham, MA, USA
Microscope slides Superfrost plus	Thermo Scientific Waltham, MA, USA
Needles 27 Gauge	BD Biosciences, San Jose, CA, USA
PCR reaction tube 0.5 ml	Biozym Scientific, Oldendorf, Germany
PCR sealers Microseal 'B' Film	BioRad, Hercules, CA, USA
Pipette tips with and without filter	Sarstedt, Nuembrecht, Germany
Reaction tubes 0.5ml, 1.5ml, 2ml	Sarstedt, Nuembrecht, Germany
Serological pipettes	Greiner Bio-One International AG, Kremsmuenster, Austria
Silicone sheet, 0.5mm thick	Sahlberg GmbH&Co., KG, Munich, Germany
Sterile filter Nalgene 0.25µm, 0.45µm	Thermo Scientific, Waltham, MA, USA
Syringes 1ml Omnifix	B. Braun Melsungen AG, Melsungen, Germany
Ultracentrifugation tube Ultra-Clear 25x89 mm	Beckmann&Coulter GmbH, Krefeld, Germany
X-ray film CEA RP New	Agfa Healthcare, Mortsel, Belgium

Table 2: Disposable equipments

2.3 Chemicals/reagents

Chemicals/reagents	Manufacturer
2-mercaptoethanol	Sigma-Aldrich Chemie GmbH, Munich, Germany
70 % Ethanol	BrüggemannAlcohol Heilbronn GmbH, Heilbornn, Germany
Acetic acid	Merck Chemicals GmbH, Hessen, Germany
Agarose	Thermo Scientific, Waltham, MA, USA
Ammonium persulfate (APS)	Sigma-Aldrich Chemie GmbH, Munich, Germany
Ampicillin	Sigma-Aldrich Chemie GmbH, Munich, Germany
Boric acid	Sigma-Aldrich Chemie GmbH, Munich, Germany
Bovine serum albumin (BSA)	Sigma-Aldrich, St. Louis, MO, USA
Bromophenol blue	Serva Electrophoresis GmbH, Heidelberg, Germany
Calcium chloride	Merck Chemicals GmbH, Hessen, Germany
Chlorophorm	Sigma-Aldrich Chemie GmbH, Munich, Germany
Citric acid	Sigma-Aldrich Chemie GmbH, Munich, Germany
Color Prestained Protein Standard, Broad Range (11–245 kDa)	New England Biolabs GmbH, Frankfurt, Germany
COMPLETE™, Mini protease inhibitor cocktail	Roche, Basel, Switzerland
Dimethyl sulfoxide (DMSO)	Sigma-Aldrich Chemie GmbH, Munich, Germany
Dithiothreitol (DTT)	Cell-Signaling, Cambridge, England
DNA ladder (100 bp and 1000 bp)	New England Biolabs GmbH, Frankfurt, Germany
DNA loading buffer (6 x)	Thermo Scientific, Waltham, MA, USA
Dulbecco's Modified Eagle's Medium	Biochrom, Merck Millipore, Berlin, Germany

(DMEM)	
E. coli, DH10B	PD Per Sonne Holm, Experimental Urology, Klinikum rechts der Isar, TUM
Ethanol absolute	Merck Chemicals GmbH, Hessen, Germany
Ethidiumbromide 10 mg/ml	Sigma-Aldrich Chemie GmbH, Munich, Germany
Ethylenediaminetetraacetic acid (EDTA), 0.5 M	AppliChem, Darmstadt, Germany
FastAP phosphatase	Thermo Scientific, Waltham, MA, USA
Fetal Bovine Serum (FBS)	Biochrom, Merck Millipore, Berlin, Germany
Formaldehyde (36.5 – 38 %)	Sigma-Aldrich Chemie GmbH, Munich, Germany
Fugene HD	Promega Corporation, Madison, WI, USA
Glycine	Sigma-Aldrich Chemie GmbH, Munich, Germany
GoTaq ® qPCR master mix	Promega, Madison, WI, USA
GoTaq ® Green PCR master mix	Promega, Madison, WI, USA
HEPES	Sigma-Aldrich Chemie GmbH, Munich, Germany
Hydrogen chloride (HCl)	Merck Chemicals GmbH, Hessen, Germany
Hydrogen peroxide	Merck Chemicals GmbH, Hessen, Germany
Isocitrate monohydrate	Sigma-Aldrich Chemie GmbH, Munich, Germany
Isopropanol	Sigma-Aldrich Chemie GmbH, Munich, Germany
L-Glutamin 200mM	Sigma-Aldrich Chemie GmbH, Munich, Germany
Lipofectamine RNAimax	Invitrogen, Carlsbad, CA, USA
Luminol	Sigma-Aldrich Chemie GmbH, Munich, Germany
Magnesium Chloride	Sigma-Aldrich Chemie GmbH, Munich, Germany
Methanol	Sigma-Aldrich Chemie GmbH, Munich, Germany

Non-essential amino acids (NEAA)	Biochrom, Merck Millipore, Berlin, Germany
Opti-MEM	Biochrom, Merck Millipore, Berlin, Germany
p-Coumaric acid	Sigma-Aldrich Chemie GmbH, Munich, Germany
Penicillin/Streptomycin	Sigma-Aldrich Chemie GmbH, Munich, Germany
Phosphate buffered saline (PBS)	Biochrom, Merck Millipore, Berlin, Germany
Phosphotase inhibitor Mix II	Serva Electrophoresis GmbH, Heidelberg, Germany
Phusion High-Fidelity PCR Master Mix	Thermo Scientific, Waltham, MA, USA
Polybrene	Sigma-Aldrich Chemie GmbH, Munich, Germany
Potassium chloride	Merck Chemicals GmbH, Hessen, Germany
Potassium hexacyanoferrate(II) trihydrate	Sigma-Aldrich Chemie GmbH, Munich, Germany
Potassium hexacyanoferrate(III)	Sigma-Aldrich Chemie GmbH, Munich, Germany
Puromycin	Sigma-Aldrich Chemie GmbH, Munich, Germany
Restriction enzyme buffers	New England Biolabs GmbH, Frankfurt, Germany
Restriction enzymes	New England Biolabs GmbH, Frankfurt, Germany
Roswell Park Memorial Institute medium (RPMI)	Biochrom, Merck Millipore, Berlin, Germany
Rotiphorese® gel 30	Carl Roth, Karlsruhe, Germany
Select agar	Sigma-Aldrich Chemie GmbH, Munich, Germany
Skimmed milk powder	Nestlé, Vevey, Switzerland
Sodium acetate	Merck, Darmstadt, Germany
Sodium azide	Sigma-Aldrich Chemie GmbH, Munich, Germany
Sodium chloride	Merck Chemicals GmbH, Hessen, Germany

Sodium dodecyl sulfate (SDS)	Sigma-Aldrich Chemie GmbH, Munich, Germany
Sodium orthovanadate	Sigma-Aldrich Chemie GmbH, Munich, Germany
Sodium phosphate dibasic	Merck Chemicals GmbH, Hessen, Germany
Sulforhodamin B (SRB)	Sigma-Aldrich Chemie GmbH, Munich, Germany
T4 DNA Ligase	Thermo Scientific, Waltham, MA, USA
Tetramethylethylenediamine (TEMED)	Carl Roth, Karlsruhe, Germany
Trichloroacetic acid	Sigma-Aldrich Chemie GmbH, Munich, Germany
Tris(hydroxymethyl)-aminomethan	Merck Chemicals GmbH, Hessen, Germany
Triton X100	Sigma-Aldrich Chemie GmbH, Munich, Germany
Trypan blue	Biochrom, Merck Millipore, Berlin, Germany
Trypsin/EDTA	Biochrom, Merck Millipore, Berlin, Germany
Tween-20	Serva Electrophoresis GmbH, Heidelberg, Germany
X-Gal	Sigma-Aldrich Chemie GmbH, Munich, Germany

Table 3: Chemicals/reagents

2.4 Commercial kits or assays

Commercial kits or assays	Source
CellTiter-Blue® Cell Viability Assay	Promega, Madison, WI, USA
Click-iT™ EdU Alexa Fluor™ 488 Imaging Kit	Thermo Scientific, Waltham, MA, USA
High capacity cDNA reverse transcription kit	Thermo Scientific, Waltham, MA, USA
HiSpeed® Plasmid Midi Kit	Qiagen, Hilden, Germany
mirVANA miRNA isolation kit	Thermo Scientific, Waltham, MA, USA

Pierce™ BCA Protein Assay Kit	Thermo Scientific, Waltham, MA, USA
QIAprep® Spin Miniprep Kit	Qiagen, Hilden, Germany
QIAquick gel extraction kit	Qiagen, Hilden, Germany

Table 4: Commercial kits or assays

2.5 Buffer

Buffer	Components
0.2 M Citric acid/sodium phosphate buffer	36.85 ml of 100 mM citric acid 63.15 ml of 200 mM sodium phosphate dibasic pH=6
0.5 % (W/V) SRB staining solution	0.5 % SRB in 1 % acetic acid
1 % SDS Protein lysis buffer (REFERENCE)	1 % SDS 10 mM Tris/HCl, pH=7.2 1 mM sodium orthovanadate 1 Complete Mini-Protease Inhibitor tablet and 100 ul of phosphatase inhibitor were added to 10 ml of lysis buffer before use
10 x SDS page running buffer (10 x TGS)	25 nM Tris 192 mM Glycine 0.1 % w/v SDS
10 x TBE	1 M Tris 1 M Boric acid 0.02 M EDTA
10 x TBS	0.5 M Tris-HCl, pH=7.6
10 x Transfer buffer	25 nM Tris 192 mM Glycine 20 % Methanol
100 % TCA	0.3 M TCA in 22.7 ml dH2O
2 x HBS	8 g sodium chloride 0.38 g potassium chloride 0.1 g sodium phosphate dibasic

	5 g hepes 1 g glucose Add deioneizd water to 500ml, adjust pH to 7.05
4 x Protein loading buffer	0.25 M Tris-HCl, pH=6.8 8 % SDS 0.04 % Bromophenol blue 40 % Glycerine The above solution and 1 M DTT were mixed with a ratio of 5 to 1 before use
Chemiluminescence reagent	Chemiluminescence reagent part A and B were mixed with a ratio of 1 to 1 before use
Chemiluminescence reagent part A	0.1 M Tris-HCl, pH=8.5 2.5 mM Luminol 0.4 mM p-Coumaric acid
Chemiluminescence reagent part B	0.1 M Tris-HCl, pH=8.5 0.18 % hydrogen peroxide
Immunoblotting antibody dilution buffer	5 % BSA and 0.02 % sodium azide in TBS-T
Immunoblotting blocking solution	5 % skimmed milk powder in TBS-T
SA-BGal staining solution	2 ml of 0.2 M Citric acid/sodium phosphate buffer 0.5 ml of 100 mM Potassium hexacyanoferrate(II) 0.5 ml of 100 mM Potassium hexacyanoferrate(III) 300 ul of 5 M sodium chloride 20 ul of 1 M Magnesium Chloride 0.5 ml of fresh-made 20 mg/ml 6.18 ml of deionized water
Separating gel buffer	1.5 M Tris-HCl, pH=8.8
Stacking gel buffer	0.5 M Tris-HCl, pH=6.8
TBS-T	0.1 % Tween-20 in 1 x TBE

Table 5: Buffer

2.6 Antibodies

Antibodies	Dilution	Source
CDK2, 2546	1:1000	CST, Beverly, MA, USA
cyclin D1, 2978	1:1000	CST, Beverly, MA, USA
cyclin E2, 4132	1:1000	CST, Beverly, MA, USA
E2F1	1:200	Santa Cruz Biotechnology, INC., Dallas, TX, USA
E2F2, ab138515	1:2500	Abcam, Cambridge, UK
E2F3,PG37	1:100	Thermo Scietific, Waltham, MA, USA
E2F4, WUF10	1:100	Thermo Scietific, Waltham, MA, USA
E2F5, sc-999	1:100	Santa Cruz Biotechnology, INC., Dallas, TX, USA
GAPDH, 2118	1:1000	CST, Beverly, MA, USA
HA-Tag (6E2), 2367	1:1000	CST, Beverly, MA, USA
MDM2, AF1244	1 ug/ml	R&D Systems, Minneapolis, MN, USA
p107, ab209546	1:1000	Abcam, Cambridge, UK
p130, ab76234	1:1000	Abcam, Cambridge, UK
p21, 2947	1:1000	CST, Beverly, MA, USA
p27, 3686	1:1000	CST, Beverly, MA, USA
Peroxidase conjugated anti-mouse IgG, 715-036-150	1:10000	Dianova GmbH, Hamburg, Germany
Peroxidase conjugated anti-rabbit IgG, 711-036-152	1:10000	Dianova GmbH, Hamburg, Germany
pRb (Ser780), D59B7	1:1000	CST, Beverly, MA, USA
Rb, 554136	2 µg/ml	BD Bioscience, San Jose, CA, USA

Table 6: Antibodies

2.7 Primers

All primers were synthesized by Life Technologies (Darmstadt, Germany) and dissolved in DNase-free water to 10 uM stock solutions.

Target gene	Forward primer	Reverse primer
RB1	AGCAACCCTCCTAAACCACT	TGTTTGAGGTATCCATGCTATCA
GAPDH	TGGCATGGACTGTGGTCATGAG	ACTGGCGTCTTCACCACCATGG

Table 7: Primers for RT-qPCR

Primers for cloning and sequencing pCMV HA hRB-C42

Name	Primer sequence
RB1 866 Fw	CCAGACCCAGAAGCCATTGAAATC
RB1 866 EcoRV Rev	GAGATGGATATCCTAATCTGCTTCATCTGATCCTTC
RB1 3'UTR EcoRV Fw	GGTGATGATATCGGACAAACCACAACTAGAATGC
RB1 3'UTR Rev	GTGAGCGGATAACAATTTCACAC

Table 8: Primers for cloning and sequencing pCMV HA hRB-C42

2.8 Plasmid

Plasmids	Source
pcDNA 3.1 V5 His TOPO	Life Technologies, Darmstadt,Germany
pRK5-HA-Ubiquitin-WT	from Ted Dawson (Addgene plasmid # 17608) (K. L. Lim et al., 2005)
pRK5-HA-Ubiquitin-K48R	from Ted Dawson (Addgene plasmid # 17604) (K. L. Lim et al., 2005)
pCMV HA hRB-wt	from Steven Dowdy (Addgene plasmid # 58905) (Narasimha et al., 2014)
pCMV HA hRB-C42	Cloned by Qi Pan
pCMV HA hRb delta CDK	from Steven Dowdy (Addgene plasmid # 58906) (Narasimha et al., 2014)
psPAX2	from Didier Trono (Addgene plasmid # 12260)

pMD2.G	from Didier Trono (Addgene plasmid # 12259)
scramble shRNA	from David Sabatini (Addgene plasmid # 1864) (Sarbassov, Guertin, Ali, & Sabatini, 2005)
pLKO-RB1-shRNA-19	from Todd Waldman (Addgene plasmid # 25640) (Michaud et al., 2010)
pLKO-RB1-shRNA-63	from Todd Waldman (Addgene plasmid # 25641) (Michaud et al., 2010)

Table 9: Plasmids

2.9 siRNA

Target gene	Sequence of siRNA	Source
MDM2	CTCTGTCTTAAATGAGAAGTA	Qiagen, Hilden, Germany
MDM2	AATCATCGGACTCAGGTACAT	Qiagen, Hilden, Germany
Negative control	Stealth RNAi™ siRNA Negative Control Hi GC Duplex #2	Life technologies, Darmstadt, Germany
E2F1siPOOL	pools of 30 siRNAs	siTOOLs Biotech, Planegg/Martinsried, Germany
Negative ctrl siPOOL	pools of 30 siRNAs	siTOOLs Biotech, Planegg/Martinsried, Germany

Table 10: siRNA

2.10 Small molecule inhibitors

Small molecule inhibitors	Source
Roscovitine	Sigma-Aldrich Chemie GmbH, Munich, Germany
PD-0332991	Sigma-Aldrich Chemie GmbH, Munich, Germany
MG-132	Sigma-Aldrich Chemie GmbH, Munich, Germany
Epoxomicin	Sigma-Aldrich Chemie GmbH, Munich, Germany

Table 11: Small molecule inhibitors

3. Methods

3.1 Cell culture

Bladder cancer cell lines T24 (from American type culture collection, Manassas, VA, USA) and RT112 (from Leibniz Institute German collection of microorganisms and cell culture, Braunschweig, Germany) were cultured in RPMI medium containing 10% FBS, 1% NEEA and 1% penicillin/streptomycin at 37 ℃ in 5 % CO_2. HEK 293T (a gift from Dr. Per Sonne Holm, Department of Urology, TUM, Munich, Germany) were cultured in DMEM medium containing 10% FBS, 1% NEEA and 1% penicillin/streptomycin at 37 ℃ in 5 % CO_2. Cells were passaged before reaching confluence. All buffer and medium for cell culture were pre-warmed to 37 ℃ before use. Cells were washed with PBS buffer and then incubated with trypsin at 37°C for 1 – 5 minutes. Once the cells rounded up and dissociated, fresh medium was added immediately to take the cells into suspension and neutralize the trypsin. Cells were centrifuged at 300 RCF for 5 minutes, resuspended and seeded into new 10 cm plates with a dilution of 1:10 to 1:2.

Counting of cells: Cell suspension was diluted in equal volume of trypan blue and cell number was counted in Neubauer chamber. Only unstained cells were counted as viable cells.

For preservation of cells, their pellets were resuspended in freezing medium that made up of 10 % DMSO and 50 % FBS. 1 ml of freezing medium containing 5 x 10^6 cells were transferred into cryovials and stored in freezing containers at -80 ℃ for 24 hours before they were transported to liquid nitrogen for long term stock. To thaw frozen cells, the cryovial was incubated at 37 ℃ in a water bath for an immediate thawing of frozen medium. Cells were washed and then resuspended with 10 ml fresh medium before they were seeded into a 10 cm plate.

3.2 Treatment of Cells

PD-0332991 were dissolved in deioneizd water and stored as 10 uM stock solutions at -20℃. MG-132 and epoxomicin were dissolved in DMSO and stored respectively as 100 uM and 10 uM stock solution at -20 ℃. 0.5-1x10^6, 0.5-1x10^5, 0.5-1x10^4 or

500-1000 cells were seeded in 10 cm, 6 well, 12 well or 96 well plates respectively one day before treatment. Concentrations of inhibitors were made fresh in pre-warmed medium. For inhibitors dissolved in DMSO, highest DMSO concentration was used as a control.

3.3 Cell viability

The sulforhodamine B (SRB) assay was used for cell viability assay. 5 000 to 20 000 cells were seeded into 12-well plates one day before treatment. After a period of incubation time, cells were fixed with 10% (wt/vol) trichloroacetic acid for 1 hour on ice. Then the plates were rinsed gently with tap water and air-dried. The fixed cells were stained with 500 ul of 0.05% (wt/vol) SRB solution for 20 minutes. The plates were rinsed five times with 1% (vol/vol) acetic acid to remove the unbound dye. The plates were air-dried, followed by adding 1ml of 10 mM Tris-base to each well. The plates were shaked gently for 10 minutes to thoroughly solubilize the bound dye. The dissolved dye solution was diluted to 1:5 with 10mM Tris-base buffer in 96-well plates. The absorbance at 560 nm (or 510 nm if reading values were too high) was measured in a microplate reader.

3.4 Cell cycle analysis

Edu incorporation assay was used for cell cycle analysis. Click-it EdU Alexa Fluor 488 flow cytometry kit was used according to manufacturer's protocol. Briefly, cells were incubated with10 uM Edu for 2 hours and then fixed with pre-cold 75 % ethanol at -20 ℃ for at least 1 hour. Flow cytometry was performed by using fluorescence-activated cell sorting (FACS) and CellQuest software. FlowJo software (FlowJo LLC, Ashland, OR, USA) was used for analysis of data.

3.4 Immunoblot

3.4.1 Lysis of cells

Entire experiment was performed on ice. Cells were washed twice with pre-cold PBS. 500 ul or 100 ul of 1% SDS lysis buffer was added to 10 cm or 6 well plates, respectively. Cell lysates were transferred to microcentrifuge tubes. 27 gauge needles and syringes were used for shearing DNA until viscosity was invisible. The

samples were centrifuged at 33 000 RCF for 30 minutes at 4 ℃. The supernatants were used for further experiments or stored at -80 ℃.

3.4.2 Protein quantification and sample preparation

BCA protein assay was used to measure protein concentration of lysates according to manufacturer's protocol in 96-well plates. Briefly, 10 ul of protein samples or a series of protein standards were mixed with 90 ul of working reagent and incubated for 30 minutes at 37 ℃. Absorbance at 560 nM was detected and the protein concentration of the protein samples was calculated based on the reading values of protein standards. All samples were diluted to equal protein concentration with lysis buffer and then mixed with 4 x protein loading buffer containing DTT. Samples were heated at 100 ℃ for 10 minutes for denaturation and can be stored at -20 ℃.

3.4.3 Sodium dodecyl sulfate polyacrylamide gel electrophoresis (SDS-PAGE)

Separating and stacking gel solutions were prepared as described in Table. After complete polymerization, 10 ul of molecular weight markers or 40 ul of protein samples were loaded into the wells of SDS- PAGE gel. Electrophoresis was performed at 90 V for 20 minutes and then continued at 150 V until the loading front moved to the bottom of gels.

Ingredient	**8 %**	**10 %**	**12 %**
H_2O [ml]	4.78	4.12	3.45
1.5M Tris pH 8.8[ml]	2.5	2.5	2.5
30% acrylamide/Bis-acrylamide solution [ml]	2.67	3.33	4
10% APS [µl]	50	50	50
TEMED [µl]	10	10	10
Total [ml]	10	10	10

Table 12: Recipe for separation gel

Ingredient	
H_2O [ml]	3.07
0.5M Tris pH 8.8 [ml]	1.25

30% acrylamide/Bis-acrylamide solution [ml]	0.65
10% APS [µl]	25
TEMED [µl]	5
Total [ml]	5

Table 13: Recipe for stacking gel

3.4.4 Transferring the protein to the membranes

The gels were incubated in 1 x transfer buffer for 10 minutes and the PVDF membranes were incubated in methanol for 5 minutes. After incubation, the PVDF membrane was washed extensively in the transfer buffer. The gels and membranes were assembled into transfer sandwiches. Then they were inserted into cassettes and placed into transfer tanks, with the membranes on the cathode and the gels on the anode. Transfer was performed at 4 ℃ for 1 - 2 hours at 100 V.

3.4.5 Immunodetection

The membranes were blocked with blocking buffer for 1 hour at room temperature, followed by an incubation with primary antibody solution overnight at 4 ℃. The primary antibody was collected for further use (up to 5 times). Membranes were washed with TBST buffer three times and then incubated with secondary antibody solution for 1 hour at room temperature. The membranes were washed with TBST buffer three times and incubated with Chemiluminescence reagent for 2 minutes. Chemiluminescent signals were captured using autoradiography films. Image J software was applied for the quantification of target bands.

3.5 Transfection of siRNA or DNA

Transfection of siRNA was performed using Lipofectamine RNAiMax according to manufacturer's protocol. Briefly, 0.5 x 10^6 or 1 x 10^6 cells were reverse transfected in 6-well plates with a final siRNA concentration of 1 nM. Transfection of DNA was performed using Fugene HD according to manufacturer's protocol. Briefly, 1 ug of DNA mixed with 3 ul of Fugene reagent were applied to cells in 6-well plates. Medium were changed after 24 hours of transfection. All siRNA/DNA and transfection reagent complexes were prepared in Opti-MEM.

3.6 Construction of expression plasmids

3.6.1 Preparation of competent bacteria

E.coli. DH10B was incubated with 5 ml of LB medium in a shaker at 37 ℃ for 12-16 hours. 100 ul of this culture was incubated with 100 ml of LB medium in a shaker at 37 °C for 2-3 hours, followed by an incubation on ice for 30 minutes. After a centrifugation for 10 minutes at 4 ℃ with 3000 RCF, DH10B was resuspended in 35 ml of pre-cold 0.1 M $CaCl_2$. The above incubation and centrifugation were performed again. DH10B were resuspended in 1 ml of pre-cold 0.1 M CaCl2 containing 10 % Glycerol. Competent DH10B were aliquoted in pre-cold tubes and stored at -80 ℃.

3.6.2 Isolation of plasmid DNA

DNA extraction was performed according to manufacturer's protocol. In brief, the single colonies of transformed DH10B were expanded in LB medium containing selective antibiotic with vigorous shaking for 12-16 hours at 37 ℃. 5 ml (miniprep kit) or 50 ml (midiprep kit) of the bacteria culture was used for further DNA extraction respectively. DNA was dissolved in deionized water and the concentration was detected using NanoDrop 2000c. DNA solution was stored at -20 ℃.

3.6.3 Amplification of inserted sequence

PCR components were mixed in 20 ul of reaction consisted of Phusion Master Mix (Thermo Scientific, Waltham, MA, USA), 10 ng of plasmid, 0.5 uM forward and reverse primers according to manufacturer's protocol. The cycling condition was set up as follows: 1) 98 ℃ for 30 seconds. 2) 98 ℃ for 10 seconds, 62 ℃ for 10 seconds and 72 ℃ for 15 seconds /kb in 35 cycles. 3) 98 ℃ for 60 seconds.

3.6.4 Restriction digestion

For analysis of plasmid map or acquisition of specific DNA fragments, 1 ug DNA was digested with 1ul of required enzymes in 10 ul of compatible buffer at 37 ℃ overnight. The reaction was heated at certain temperature for 30 minutes for inactivation of enzyme activity. For confirming DNA sequence of plasmids, sequencing was carried

out by GATC Biotech AG, Constance, Germany. The outcomes from the sequencing were analyzed by Vector NTI Software (Thermo Scietific, Waltham, MA, USA).

3.6.5 Agarose gel electrophoresis

Agarose was dissolved in TBE buffer using microwave to form 0.8 - 2% agarose gels containing 0.5 ug/ml ethidium bromide. DNA was mixed with 6 x loading dye and loaded into gels. Electrophoresis was performed in TBE buffer at 70 V until the DNA was shifted into the gel and continued at 120 V. UV transillumination and Chemidoc XRS system were used to visualize and record DNA fragments of interest.

3.6.6 Gel extraction, dephosphorylation, ligation and transformation

Following electrophoresis, digested plasmids and inserted DNA fragments were isolated using the Qiaquick gel extraction kit according to manufacturer's protocol. FastAP phosphatase was used to dephosphorylate the ends of digested plasmids according to the manufacturer's manual. The dephosphorylation was performed at 37 ℃ for 10 minutes, followed by a heat inactivation at 65 °C for 15 minutes. For ligation, 80 fmol of the inserted fragments and 16 fmol of the digested plasmids were incubated with 1 ul of T4 DNA ligase in 10 ul of reaction at room temperature for 1 hour. 50 ul of competent DH10B was thawed on ice before transformation. 5 ul of the ligation system was added to the competent DH10B and incubated on ice for 10 min, followed by an immediate incubation at 42 ℃ for 45 seconds. After another incubation on ice for 10 minutes, the competent DH10B was mixed with pre-warmed 500 ul of LB medium and incubated in a shaker at 37 ℃ for one hour. 100 – 500 ul of the culture were evenly distributed onto pre-warmed LB agar plates containing selective antibiotic and incubated at 37 ℃ overnight.

3.6.7 PCR screening of clones

PCR mixture was prepared with GoTaq Green PCR master mix. Each single colony was picked using a sterile pipette tip and dipped into 20 ul of GoTaq Green PCR master mix containing 0.5 uM forward and reverse primers. The same tip was dipped into 5 ml of fresh LB medium containing the selection antibiotic in 15ml tubes. Each transformed clone was expanded with vigorous shaking for 12 - 16 hours at 37 ℃. After amplification of target DNA fragments by PCR, the samples were loaded into

agarose gel for electrophoresis. The correctly transformed clones were screened based on the size of the amplified DNA fragments. The identities of these clones were further confirmed using restriction digestion and eventually sequencing.

3.6.8 Cloning strategy for pCMV HA hRB-C42

pCMV HA hRB-C42 encodes a C-terminal 42 amino acids truncated RB1 protein. The C-terminal cDNA sequence of truncated RB1 and DNA sequence of 3' UTR were amplified using plasmid pCMV HA hRB-WT as a template. The primers for the former are RB1 866 Fw (CCAGACCCAGAAGCCATTGAAATC) and RB1 866 EcoRV Rev (GAGATGGATATCCTAATCTGCTTCATCTGATCCTTC). The ones for the latter are RB1 3'UTR EcoRV Fw (GGTGATGATATCGGACAAACCACAACTAGAATGC) and RB1 3'UTR Rev (GTGAGCGGATAACAATTTCACAC). These two fragments were ligated into the inserted fragment after their digestion by restriction enzyme EcoRV. The inserted fragment was then ligated into the backbone of pCMV HA hRB-WT using the same restriction enzyme sites NheI (Fig 3).

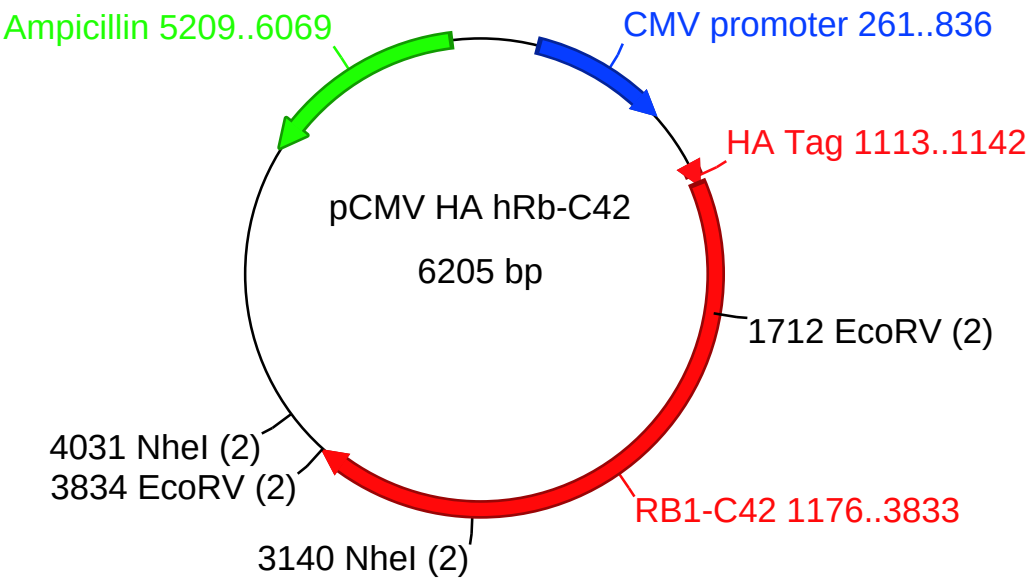

Figure 3: The map of pCMV HA hRB-C42

3.7 Knockdown of RB1 – generation of stable tranduced cell lines

3.7.1 Production of lentivirus

1.5 million HEK 293T cells were seeded into 10 cm plates for lentiviral production and transfected 24 hours after seeding. For each 10 cm plate, 20 ug of transfer DNA, 15 ug of psPASX2 and 6 ug of pMD2.G plasmids were transfected using 2.5 M $CaCl_2$ and 2 x HBS as described previously (Salmon & Trono, 2007). Medium was changed 6 hours after transfection and virus supernatant was collected at 48 hours. This supernatant was sterile filtered with a 0.45 um PVDF filter and stored at 4 ℃ for 1 week and at -80 ℃ for long term stock.

3.7.2 Transduction of cells with lentivirus

0.1, 1.5 and 4 million cells were seeded for viral transduction in 6-well, 10 cm and 15 cm plates respectively. Transduction was conducted using 8 ug/ml polybrene 24 hours after seeding. 1 ug/ml puromycin was applied to the cells 24 hours after transduction and selection pressure was continued for 7 days. Passaging of cells and medium changes were conducted as necessary. After selection, single clone was expanded in 96-well plates.

3.8 SA-βGAL staining

The assay was performed in 12-well plates as previously described (Debacq-Chainiaux, Erusalimsky, Campisi, & Toussaint, 2009). Subconfluent cells were washed gently twice with PBS and then fixed with 2% formaldehyde 0.2% glutarahdehyde solution for 5 minutes at room temperature. The fixed cells were washed with PBS twice and then incubated with 500 ul of fresh made staining solution at 37 ℃ for 12 - 16 hours. During the incubation, the plates should be sealed with parafilm and protected from light. Also, the exact and stable pH value was crucial for the reaction so that the incubator was not supplied with CO_2. The stained cells were washed twice with PBS and once with methanol. The positive cells were observed and captured with phase contrast microscopy and software Zen Lite 2012 (Carl Zeiss, Oberkochen, Germany).

3.9 Real-time reverse transcription polymerase chain reaction (RT-qPCR)

3.9.1 RNA extraction

Extraction of total RNA from adherent cells in 6-well plates was performed using the mirVANA miRNA isolation kit according to manufacturer's protocol. The purified RNA was stored at -80 ℃ before use. Dissolved in Rnase-free water, RNA concentration and quality was detected using Nanodrop 2000c. The ratio between absorbance in 260 nM and that in 280 nM (A260/A280) was used to evaluate the extent of protein contamination in RNA samples. The values between 1.8 and 2.0 were accepted for further applications.

3.9.2 cDNA synthesis

2 ug of total RNA from the above extraction was set as template for reverse transcription in a 20 ul of volume using High capacity cDNA reverse transcription kit according to manufacturer's protocol.

3.9.3 Quantitative polymerase chain reaction (qPCR)

The reaction for qPCR was prepared in a 10 ul of GoTaq qPCR Master mix with 50 ng of cDNA, 0.5 uM of forward and reverse primers. Each PCR reaction was run in triplicate in a CFX96 Real-Time PCR detection system. The cycling condition was set as follows: 94 ℃ for 2 minutes, 94 ℃ for 15 seconds, 60 ℃ for 30 seconds and 72 ℃ for 1 minute for 40 cycles. For quality control of the reaction, the melting curve from each reaction was examined first for the number of peaks. Then the amplified DNA products were loaded into agarose gel for electrophoresis to ensure the correct size of products and no formation of primer-dimer.

3.9.4 Relative quantification of gene transcription

Housekeeper gene GAPDH was used to normalize the transcription of target genes. The ΔΔCT method was used for relative quantification of gene transcription as follows (Livak & Schmittgen, 2001):

ΔCT=CT (gene of target) – CT (GAPDH)

ΔΔCT= ΔCT (treated sample) –ΔCT (control)

Relative gene expression = $2^{-\Delta\Delta CT}$

4. Result

4.1 The role of RB1 in therapy response to CDK4/6 inhibition

4.1.1 Biochemical and functional effects of CDK4/6 inhibition

To elucidate the role of RB1 in therapy response to CDK4/6 inhibitors, biochemical effects of CDK4/6 inhibition on RB1 was investigated. Treatment of cells with PD 0332991, a selective CDK4/6 inhibitor, caused a synchronous reduction of both total RB1 protein and phosphorylated RB1 in T24 and RT112 cells (Fig 4A), which correlated with robust G1 phase arrest and decrease in S (Edu positive) and G2/M phase entry(Fig 4B).

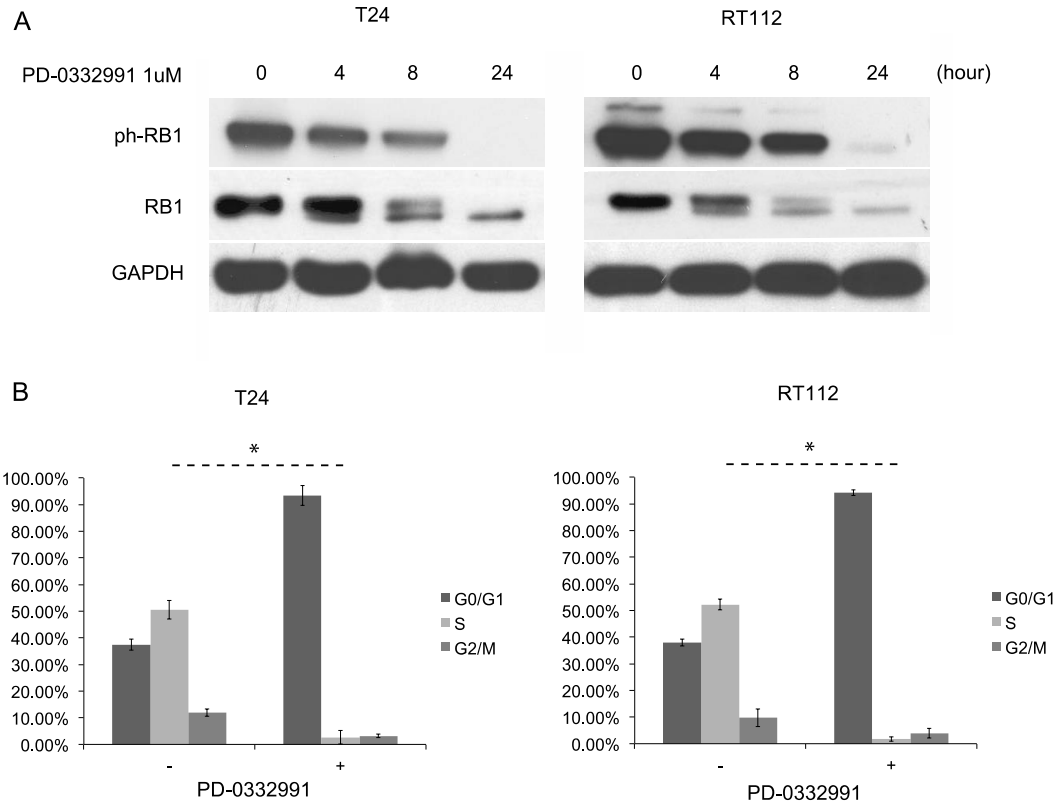

Figure 4: Decrease of total and phosphorylation of RB1 upon CDK4/6 inhibition correlates with therapy response.

(A) T24 and RT112 cells were treated with 1000 nM PD-0332991 for indicated time points. The protein level of downstream targets were detected by immunoblot. Hyper- (upper bands) and hypo- (lower bands) phosphorylated RB1 could be distinguished by 6% gel electrophoresis and detection with an RB1 antibody. (B) Treated with 1000 nM PD-0332991 for 24 hours, cell cycle progression was detected by Edu

incorporation. The graphs show the values +/- S.E. from three different experiments. “*” indicating $p<0.05$, two-tailed Student‘s T test.

4.1.2 Effects of CDK4/6 inhibition on RB1-knockdown cells

The above observations that down-regulation of RB1 correlated with therapy response to CDK4/6 inhibition seems to be contradictory to the concept that presence of RB1 is a prerequisite for therapy response. This proned us to examine the requirement of RB1 for therapy response. RB1-knockdown cell lines were established by transducing T24 with a lentivirus encoding for small haipin RNAs, shRB1-19 or shRB1-63, directed against RB1 mRNA. Three clones transduced with each of the shRNAs were analyzed for their RB1 expression level and therapy response to PD-0332991. All clones transduced with shRB1-19 and shRB1-63 showed a stable and robust decrease in RB1 expression of approximately 95%, compared to control (Fig 5A). Upon 24 hours of PD-0332991 treatment, RB1-knockdown cells still maintained a high proportion of cells that enter into S phase (30%) and G2/M phase (12%), compared to control (less than 1% in S and G2/M phases) (Fig 5B), indicating a loss of therapy response after silence of RB1. Also, incubated with PD-0332991 for 3 days, cell viability of these RB1-knockdown cells was not influenced as significantly as that of control (Fig 5C). These findings indicated that the expression of RB1 is required for therapy response to CDK4/6 inhibition.

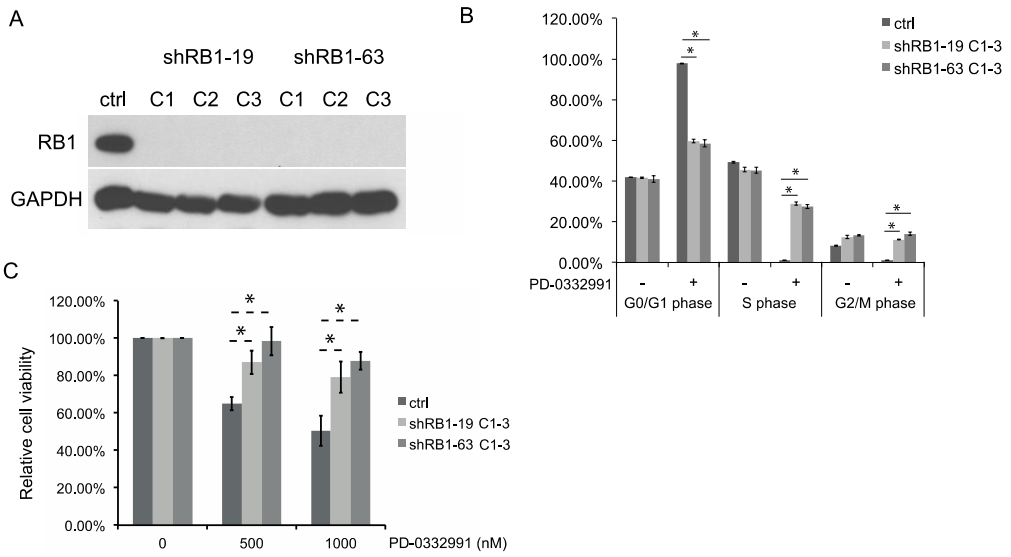

Figure 5: The expression of RB1 is required for therapy response.

(A) T24 cells were transduced with two different lentivirus shRNAs, shRB1-19 and shRB1-63, to repress RB1 expression. For each shRNA, the expression level of RB1 in three clones was detected by immunoblotting. (B) These clones were treated with 1000nM PD-0332991 for 24 hours and the proportion of cells in cell cycle phases were detected by Edu incorporation assay. (C) These clones were treated with 0, 500, 1000nM PD-0332991 for 72 hours and cell viability were detected by SRB staining. The graphs show the values +/- S.D. from three different clones. "*" indicating $p<0.05$, two-tailed Student's T test.

4.1.3 Effects of CDK4/6 inhibition on RB1 transcription

If therapy response requires expression of RB1, why is there a robust reduction of RB1 that correlates with therapy response upon CDK4/6 inhibition? We tried to explain this observation by first studying mechanisms that are involved in RB1 down-regulation upon CDK4/6 inhibition. We first confirmed previous data in which we have shown that CDK4/6 inhibition suppresses RB1 transcription (Sathe et al., 2015). Treating T24 and RT112 with 1uM PD-0332991 inhibited transcriptional level of RB1 in a time-dependent manner with a reduction of 60% and 66% respectively at 24 hour (Fig 6).

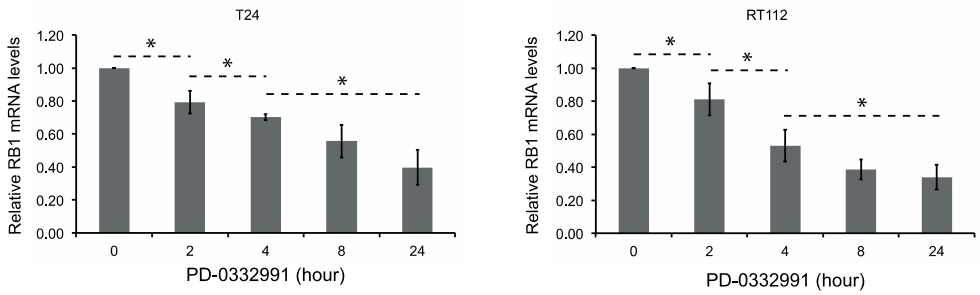

Figure 6: RB1 transcription is downregulated upon CDK4/6 inhibition.

T24 and RT112 cells were treated with 1000 nM PD-0332991 for indicated hours. The RB1 mRNA levels were detected by RT-qPCR. The graphs show the values +/- S.E. from three different experiments. "*" indicating $p<0.05$, two-tailed Student's T test.

4.1.4 The role of proteasome pathway in RB1 down-regulation upon CDK4/6 inhibition

Next we addressed if protein degradation also contributed to RB1 downregulation upon CDK4/6 inhibition. Considering that many cellular proteins are degraded by the ubiquitin-dependent proteasome pathway (Lub et al., 2015), we evaluated biochemical effects when using proteasome inhibitors upon PD-0332991 treatment. First, dose response curves for cell viability of T24 and RT112 treated for 24 hours with MG-132 and epoxomicin, which are established proteasome inhibitors, were measured. Treatment with either of proteasome inhibitors can decrease the cell viability in a dose-dependent manner, and T24 cells are more sensitive to proteasome inhibition than RT112 cells (Fig 7).

Next, cells were treated with either MG-132 or epoxomicin using different concentrations in combination with PD0332991 (1uM) and expression level of RB1 protein was detected by immunoblotting of total cell lysates. A partial rescue in the reduction of RB1 protein level could be observed in a dose-dependent manner (Fig 8A-B). Rescue of RB1 protein correlated with concentrations of the inhibitors used, when cell viability was affected by up to 20-60% (compare to Fig.7). Interestingly, an additional suppression of RB1 transcription was observed after treatment with

epoxomicin (Fig 8C), excluding the possibility that proteasome inhibition rescues down-regulation of RB1 upon PD-0332991 treatment by activating its transcription. Taken together, these observations indicated a partial involvement of a proteasome-dependent degradation mechanism of RB1 upon CDK4/6 inhibition.

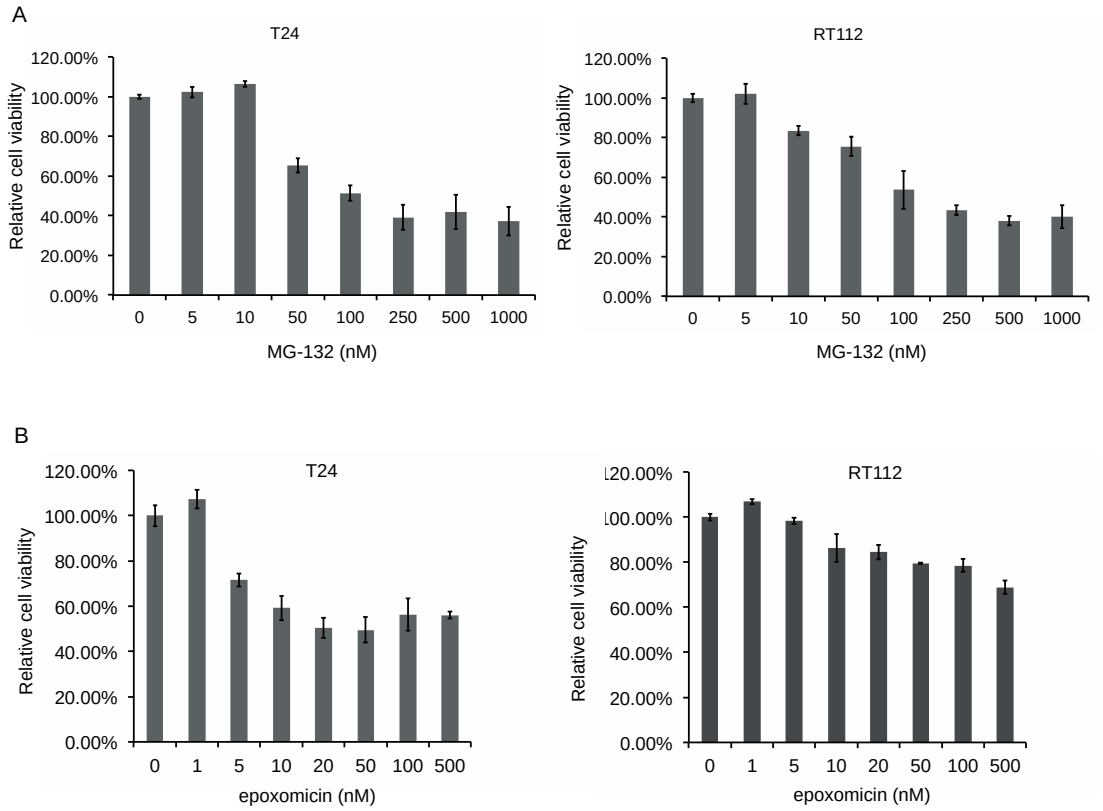

Figure 7: Dose response assay for cell viability of T24 and RT112 treated with proteasome inhibitors.

(A)(B) T24 and RT112 cells were treated with either MG-132 or epoxomicin of indicated concentrations. Cell viability was detected after 24 hours of the treatment. The graphs show the values +/- S.E. from three different experiments.

Generally, the mechanism of proteasome-mediated degradation of proteins relies on ubiquitination of target proteins. And only those proteins with a poly-ubiquitination formed on lysine 48 (K48) of ubiquitin can be recognized and degraded by the 26S proteasome (Lub et al., 2015). In order to confirm the above observation, plasmids encoding for either wild type ubiquitin (pRK5-HA-Ubiquitin-WT (Ubi-WT) or ubiquitin mutated in lysine 48 to alanine (pRK5-HA-Ubiquitin-K48R (Ubi-K48R) were used (K. L. Lim et al., 2005). The recombinant Ubi-K48R competes with endogenous wild-type

ubiquitin and prevent target proteins from poly-ubiquitination. 2 days after transfection, expression of recombinant ubiquitin was detected in immunoblots via its HA-tag (Fig 8D). However, exogenous Ubi-K48R had no evident effect on RB1 degradation after PD-0332991 treatment (Fig 8E). The probably explanation could be either that this degradation is ubiquitin independent but still proteasome dependent or that the level of the recombinant Ubi-K48R were insufficient to competitively inhibit activity of endogenous wild-type ubiquitin.

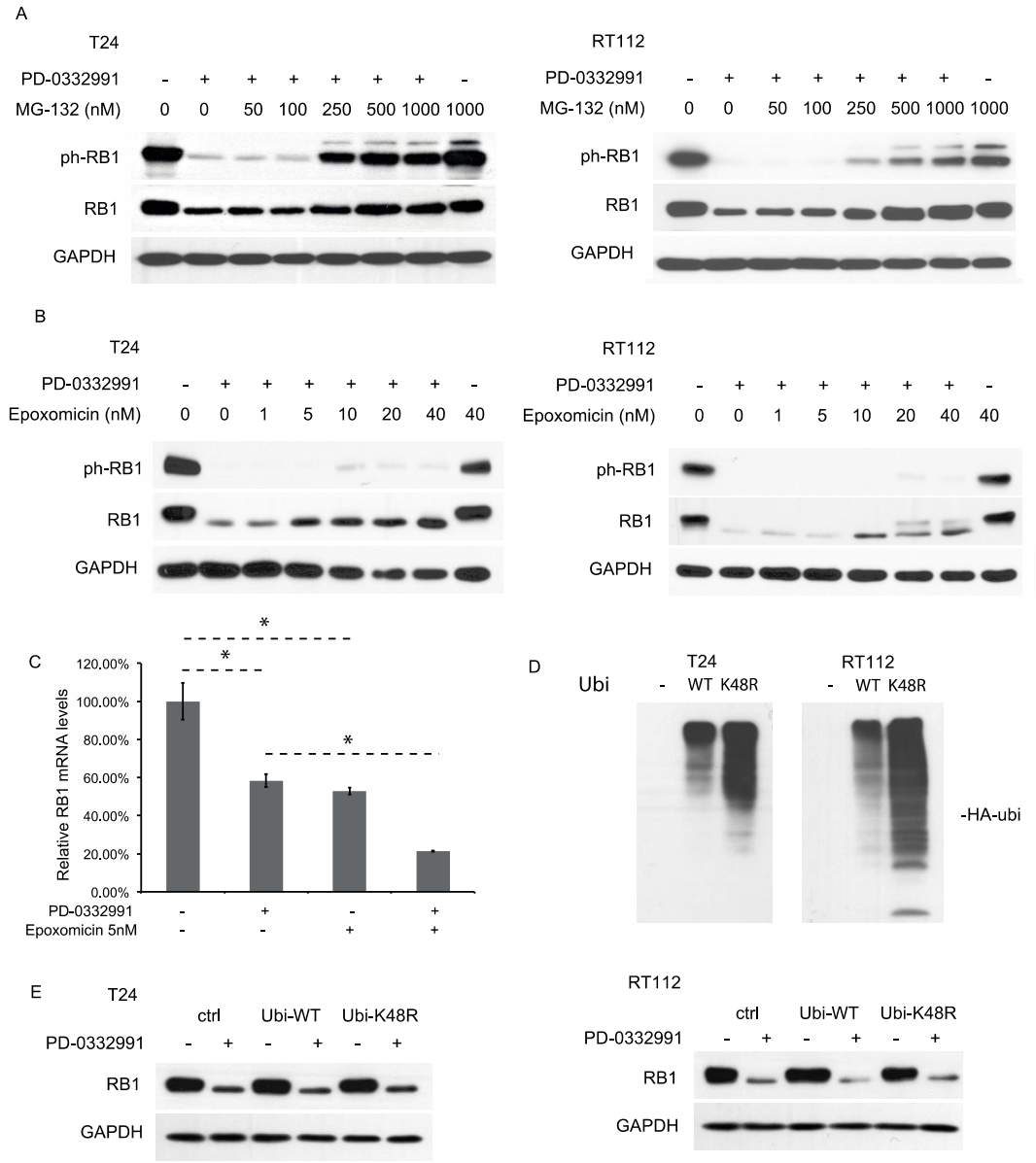

Figure 8: RB1 degradation upon CDK4/6 inhibition is proteasome dependent.

(A)(B) T24 and RT112 were treated with a combination of proteasome inhibitors (MG-132 or epoxomicin) and 1uM PD-0332991 for 24 hours. The level of RB1 and its

phosphorylation were analyzed by immunoblot. (C) T24 cells were treated with a combination of 5 nM Epoxomicin and 1uM PD-0332991 for 24 hours. Transcriptional level of RB1 was analyzed by RT-qPCR. (D) Cells were transfected respectively with pcDNA3.1 (ctrl), pRK5-HA-Ubiquitin-WT (Ubi-WT) and pRK5-HA-Ubiquitin-K48R (Ubi-K48R). After 24 hours the expression of HA tagged recombinant ubiquitin was detected by immunoblotting. (E) The above transfected cells were treated with 1uM PD-0332991 for 24 hours. The level of RB1 was analyzed by immunoblotting. The graphs show the values +/- S.E. from three different experiments. "*" indicating $p<0.05$, two-tailed Student's T test.

4.1.5 The role of MDM2 in RB1 degradation upon CDK4/6 inhibition

MDM2 is a ubiquitin-protein E3 ligase that could target RB1 for proteasomal degradation in a ubiquitin independent mechanism (Sdek et al., 2005; Uchida et al., 2005). Here we evaluated whether MDM2 is involved in RB1 degradation under CDK4/6 inhibition. Two different siRNAs were designed for silencing MDM2 expression. After transfection, the protein level of MDM2 protein in T24 and RT112 was efficiently reduced by either of the siRNAs as shown in immunoblots (Fig 9A). Knockdown of MDM2 partially prevented RB1 down-regulation upon PD-0332991 treatment in a time-dependent manner, with a robust rescue of 70% in T24 and 35% in RT112 after 8 hours of treatment. However, after 24 hours of treatment RB1 level were reduced and comparable to the control (Fig 9A). Consistent with the kinetics of RB1 level, a partial rescue of cell cycle arrest upon PD-0332991 treatment was observed in a time-dependent manner showing that a relative proportion of cells in S phase was up to 20% higher in MDM2-knockdown cells than that in control after 8 hours of treatment, while such a difference was not longer observed after 24 hours of treatment (Fig 9B). These data indicated that MDM2/proteasome-mediated RB1 degradation is another pathway that contributes for RB1 down-regulation upon CDK4/6 inhibition, apart from transcriptional repression.

It has been reported that the MDM2-binding site locates in the C-terminus of the RB1 protein (Janicke, Walker, Lin, & Porter, 1996; Sdek et al., 2004). In order to further confirm the role of MDM2 in RB1 degradation upon CDK4/6 inhibition, three HA-tagged recombinant RB1 expression plasmids were transfected into T24 and RT112,

encoding wild type RB1 (RB1- WT), mutant RB1 lacking the C-terminal 42 amino acids (RB1-C42) and mutant RB1 with all CDKs phosphorylation sites mutated (RB1-CDK). Upon PD-0332991 treatment on RT112, RB1-WT and RB1-CDK were degraded to a similar extent (Fig 9C). However, RB1-C42 showed resistance to degradation (Fig 9C), indicating that MDM2-binding, but not the status of phosphorylation is required for RB1 degradation upon CDK4/6 inhibition. Surprisingly, the three recombinant RB1 proteins above were degraded to a similar extent in T24 upon treatment (Fig 9C). Thus, MDM2 binding to RB1 seems not the only mechanism that regulates degradation of RB1 as a therapy response to CDK4/6 inhibition.

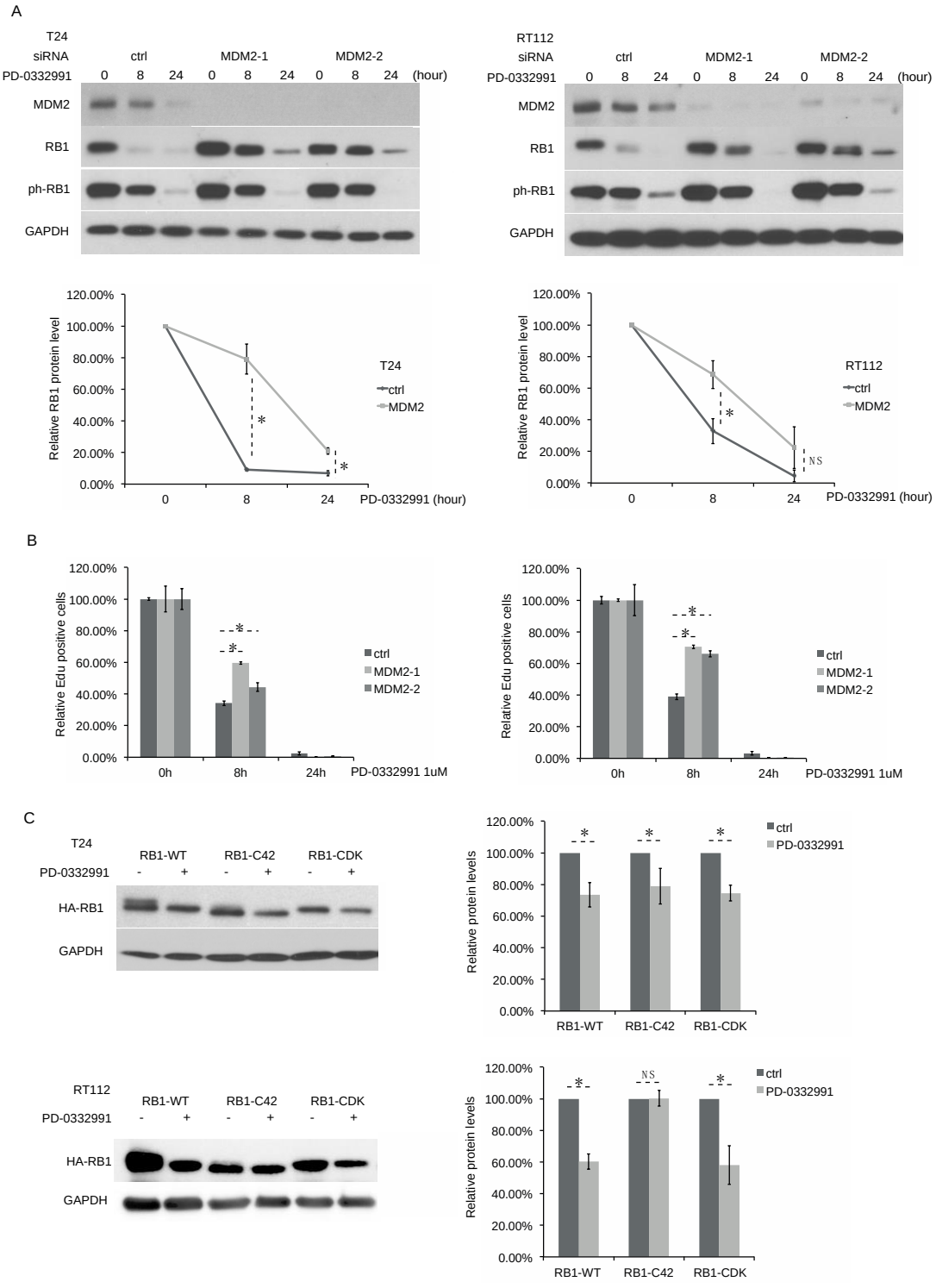

Figure 9: RB1 degradation upon CDK4/6 inhibition is MDM2 dependent

(A) (B) T24 and RT112 were transfected respectively with 1nM control siRNA (ctrl), MDM2-1 and MDM2-2 for 48 hours, followed by 1000nM PD-0332991 treatment for indicated hours. Protein levels of MDM2, RB1 and its phosphorylation were detected immunoblot. The proportion of cells in S phase was detected by Edu incorporation assay. (C) T24 and RT112 cells were transfected respectively with pCMV HA hRB-

WT (RB-WT), pCMV HA hRb delta CDK (RB-CDK) and pCMV HA hRB-C42 (RB-C42) for 24 hours, followed by an incubation of 1000nM PD-0332991 for 24h. Protein expression of HA tagged recombinant RB1 was detected by immunoblotting. All graphs show the values +/- S.E. from three different experiments. "*" indicating $p<0.05$, two-tailed Student's T test.

4.2 Partial therapy resistance to prolonged CDK4/6 inhibition

4.2.1 Long-term effects of CDK4/6 inhibition on cell viability and senescence

We are curious whether CDK4/6 inhibition has a continuous cytostatic effect on bladder cancer cells. So its long-term effect on cell viability was examined. T24 and RT112 cells were incubated with daily-changed PD-0332991 (1 uM) for up to 13 days and the relative cell number was counted by SRB staining every three days from Day 1. As expected, the proliferation rate of cells under the treatment was much lower than that of control, and the control reached a complete confluence at Day 7 (Fig 10A). However, a slow and continuous cell proliferation was still observed under prolonged treatment (Fig 10A), indicating that cell cycle progression was only partially blocked.

It has been reported that a chronic CDK4/6 inhibition can induce senescence, meaning a permanent cell cycle exit among tumor cells, although the ratio is variable and depends on the type of carcinoma and cell line studied (Acevedo et al., 2016a; Yoshida et al., 2016). Thus, we wanted to address if this effect could be also induced in bladder cancer cell lines under prolonged treatment. T24 and RT112 were incubated for two weeks with daily-changed PD 0332991 (1uM). For detecting cells that underwent senescence, we applied SA-β-Galactosidase staining that marks cells in the status of senescence. Since Day 1 of PD-0332991 treatment, morphology of cells had turned inflated (Fig 10B), which is usually observed on senescent cells. Senescent cells could showed up after 7 days of treatment, and on Day 14 the percentages of that were up to 22% among T24 cells and 45.7% among RT112 cells (Fig 10B). Taken together, senescence could be induced among a small subfraction of BC cells under prolonged CDK4/6 inhibition. However, its contribution to therapy response seems not to be substantial in BC.

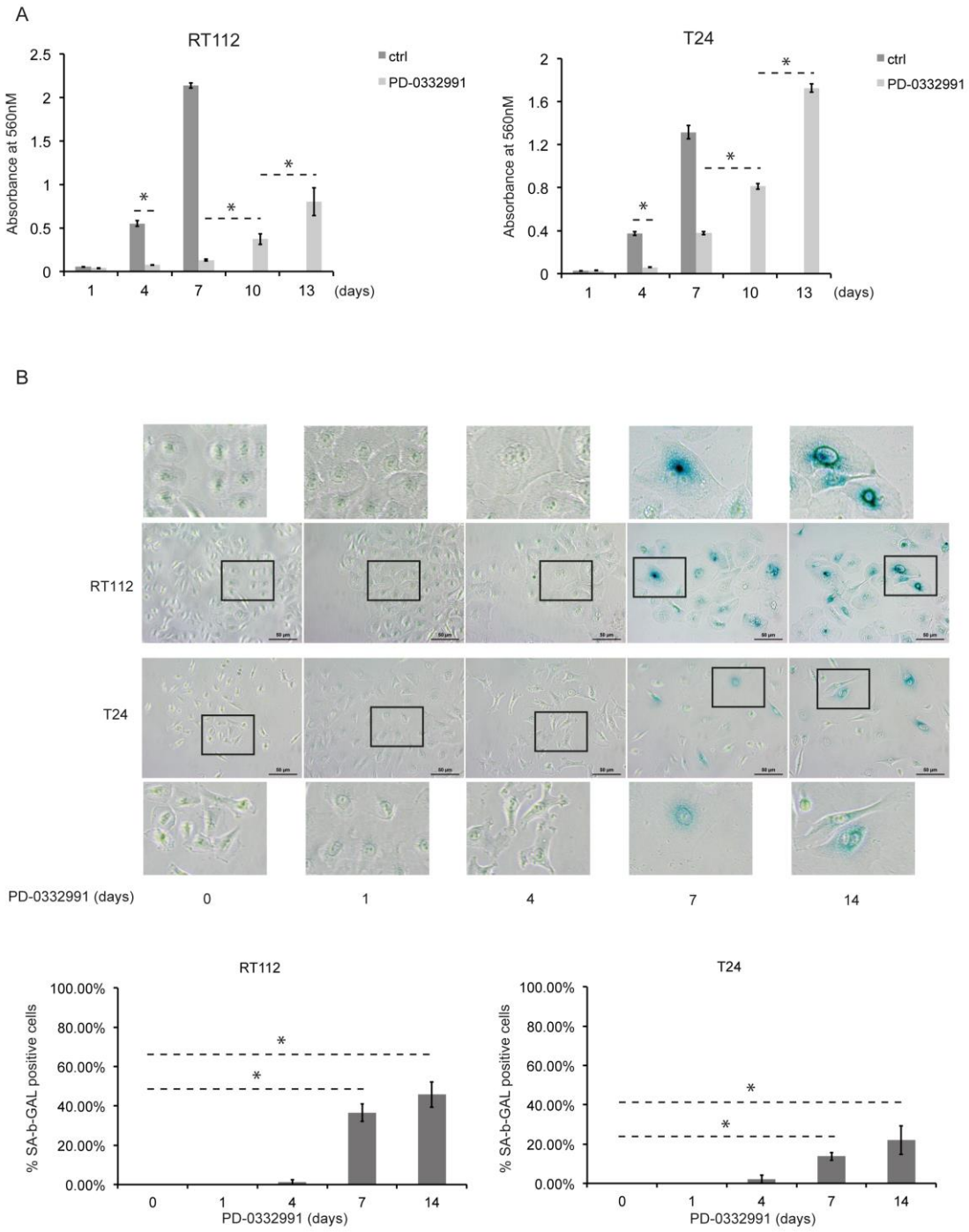

Figure 10: Insufficient cytostatic effect and senescence induction under prolonged CDK4/6 inhibition.

RT112 and T24 were treated with 1 uM daily-changed PD-0332991 for indicated days. (A) Cell viability was analyzed by SRB staining. (B) The fraction of senescent cells were detected by SA-β-Galactosidase staining. The images are the representatives from three independent experiments. The graphs show the values +/-

S.E. from three different experiments. "*" indicating p<0.05, two-tailed Student's T test.

4.2.2 Effects of prolonged CDK4/6 inhibition on cell cycle progression

A robust cell cycle arrest was observed in T24 and RT112 upon 24 hours of PD-0332991 treatment, with a decrease of cells in S stage to less than 5% (Fig 11). However, we also observed from the last cell viability assay that cell proliferation was only partially blocked under prolonged CDK4/6 inhibition (Fig 10A). This proned us to examine the status of cell cycle progression under prolonged treatment. Interestingly, a partial re-entry into G1/S transition was observed under the prolonged daily-changed PD-0332991 incubation, with the proportion of cells in S stage increasing from the initial less than 5% to around 20% at Day 2 and Day 3 (Fig 11).

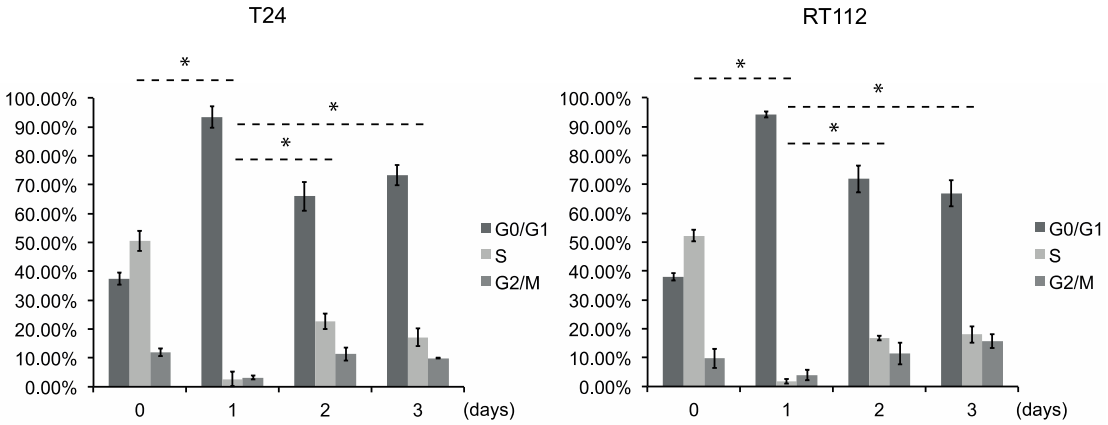

Figure 11: Partial recovery of cell cycle progression under prolonged CDK4/6 inhibition.

Edu incorporation assay of T24 and RT112 cells that were treated with 1uM daily-changed PD-0332991 for indicated days. The graphs show the values +/- S.E. from three different experiments. "*" indicating p<0.05, two-tailed Student's T test.

4.2.3 Biochemical effects of prolonged CDK4/6 inhibition

Next the downstream molecules involve in CDK4/6-RB1-E2Fs pathway were analyzed. An early decrease of total and phospho-RB1, expression level of cyclin E2

and E2F1 was observed upon PD 0332991 treatment for 1 day, followed by a partial recurrence of these molecules under prolonged treatment (Fig. 12), which correlated with the dynamic change of entry into S phase (Fig 11). In terms of the other two RB family members (p107 and p130) expression of p107 was down-regulated 2 days after treatment in T24. RT112 cells were negative for p107 expression. Expression of p130 was up-regulated in both cell lines after the first day of treatment. Besides E2F1, the levels of E2F2-5 were differentially regulated upon the treatment. It was observed in both cell lines that expression of E2F2 remained stable, while that of E2F3 reduced immediately after the first day of treatment. However, the expressions of E2F4 and E2F5 were down-regulated in T24, but were up-regulated in RT112 (Fig 12). In summary, the observations above showed that a partial recurrence of RB1 phosphorylation, E2F1 and cyclin E2 correlated with a partial recovery of cell cycle progression upon prolonged CDK4/6 inhibition.

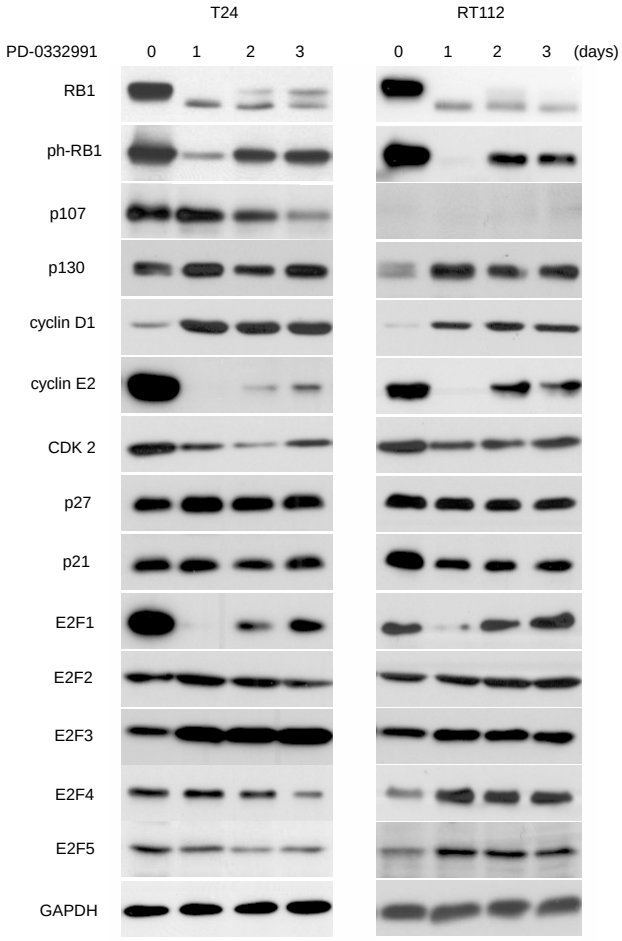

Figure 12: Differential regulation on protein levels of E2Fs and their downstream targets upon prolonged CDK4/6 inhibition.

T24 and RT112 were treated with 1 uM daily-changed PD-0332991 for indicated days. The protein levels of downstream targets were analyzed by immunoblot.

4.2.4 Combination of CDK2 and CDK4/6 inhibition display a synergistic effect

Both CDK4/6 and CDK2 are kinases that regulate RB1 phosphorylation, cyclin D activation and cell cycle progression. Whether a compensative CDK2-RB1-E2F1 pathway contributed to cell cycle re-entry under prolonged CDK4/6 inhibition was further evaluated. The dose response effect for cell viability of RT112 treated for 72 hours with roscovitine, a selective CDK2 inhibitor which mainly targets CDK2 and other kinases like CDC2 and CDK5, were determined first (Fig 13A). When cells were treated with a combination of PD-0332991 (1uM) and roscovitine (5uM) for 72 hours, the cell viability decreased by 67% compared to control (Fig 13B). The combination index (CI) was 0.69, indicating a synergistic effect from this combination therapy. Treatment with roscovitine (5uM) alone for 24 hours had very limited effect on S phase entry and RB1 phosphorylation (Fig 13C-D), indicating that physiologically cell cycle progression mainly relies on activity of CDK4/6 in these cells. Interestingly, after the treatment with PD-0332991 for 2 days, roscovitine was combined with PD-0332991 for another 24 hours, and it reduced the proportion of cells in S phase to less than 5% again (Fig 13B). Consistently, the recurrence of phosphorylated RB1, cyclin E2 and E2F1 were also suppressed by the combination with roscovitine in a dose dependent manner (Fig 13C). These data indicated that additional CDK2 inhibition prevented the re-entry of cell cycle under prolonged CDK4/6 inhibition. This might explain the synergistic effect of the two inhibitors.

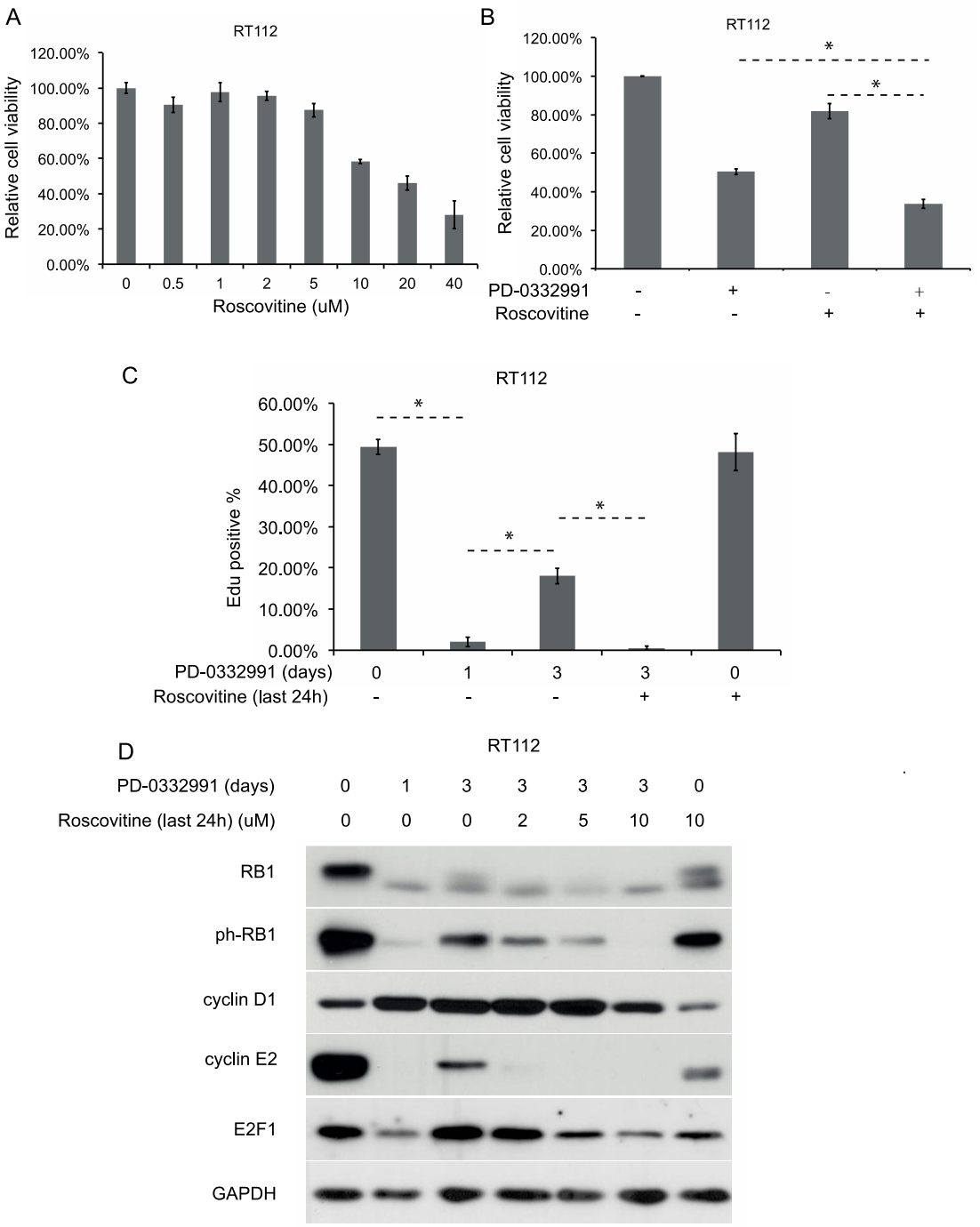

Figure 13: Partial re-entry into cell cycle under prolonged CDK4/6 inhibition is prevented by a combinative CDK2 inhibition.

(A) Dose response assay for cell viability of RT112 treated for 72 hours with roscovitine. (B) Cell viability assay of RT112 treated alone or combinatively with 1uM PD-0332991 and 5uM roscovitine for 3 days. (C) Edu incorporation assay and (D) immunoblot analysis of RT112 cells that were treated with a combination of 1uM PD-0332991 for 3 days and 5uM roscovitine for the late 24 hours. The graphs show the

values +/- S.E. from three different experiments. “*” indicating $p<0.05$, two-tailed Student‘s T test.

4.2.5 The role of E2F1 in therapy response

Based on the above finding, the level of E2F1 highly correlates with the response to CDK4/6 inhibitors. Thus, we aimed to evaluate the role of E2F1 during CDK4/6 inhibition. T24 and RT112 cells were transfected with pooled siRNA to knock down endogenous E2F1, followed by a treatment with PD-0332991 for 1 and 2 days. Surprisingly, knockdown of E2F1 did not arrest the cell cycle (Fig 14A-B). Neither did it influence the initial therapy response. Furthermore, even though the recurrence of E2F1 upon 2 days of PD-0332991 treatment was prevented by knockdown of E2F1, the cell cycle re-entry was not reversed (Fig 14A-B). Taken together, cell cycle progression and therapy response to CDK4/6 inhibition are independent of E2F1 in our model.

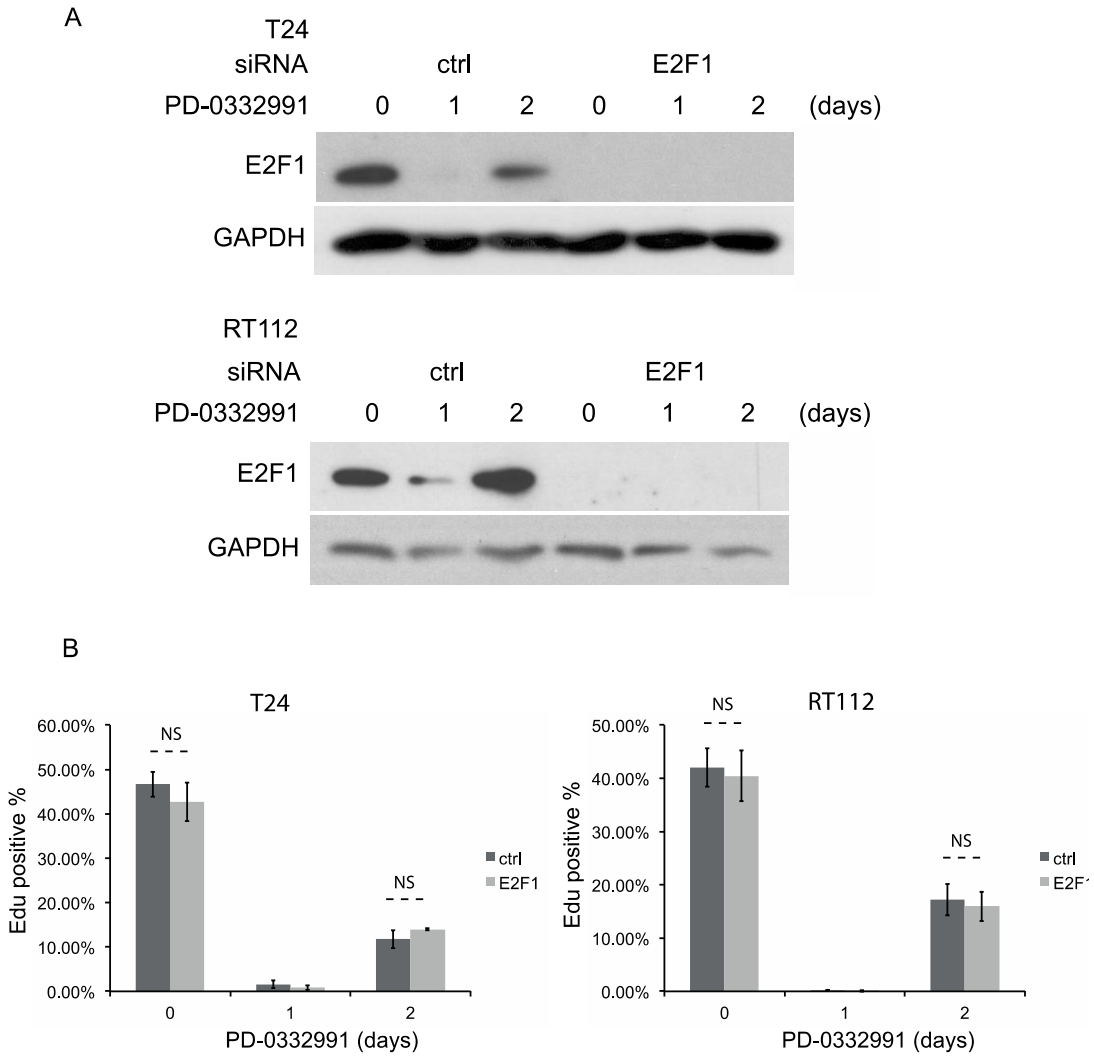

Figure 14: Cell cycle progression and therapy response to CDK4/6 inhibition are independent of E2F1.

(A) Immunoblot analysis and (B) Edu incorporation assay of T24 and RT112 cells that were transfected with 1nM control (ctrl) or E2F1 siRNA for 24 hours, followed by a treatment with1uM PD-0332991 for indicated days. The graphs show the values +/- S.E. from three independent experiments. “NS” indicating p>0.05, two-tailed Student‘s T test.

5. Discussion

Our previous preclinical study has demonstrated that CDK4/6 is a potential therapy target in RB1 positive BC cells. In this project, we studied molecular mechanisms underlying therapy response to CDK4/6 inhibition by PD-0332991, especially focusing on the down-regulation of RB1 and its implication for therapy response. Results in this work have demonstrated that the expression of RB1 is required for therapy response. However, both transcriptional repression and MDM2-dependent proteasomal degradation are involved in this down-regulation of RB1, which is also an indicator of therapy response. In addition, analysis on the functional and biochemical effects of prolonged CDK4/6 inhibition revealed that a partial recovery of cell cycle progression and re-phosphorylation of RB1 under prolonged treatment.

5.1 Down-regulation of RB1 upon CDK4/6 inhibition

According to the classical model of the CDK4/6-RB1 pathway, RB1 is a key downstream target for CDK4/6 inhibition, since its phosphorylation from kinases CDK4/6 is suppressed. In this project and in our previous work (Sathe et al., 2015) we have demonstrated that treatment of the BC cell lines T24 and RT112 with a selective CDK4/6 inhibitor, PD-0332991, caused a decrease in expression level of total and phosphorylated RB1 as well as transcription of E2F target genes correlated with a G0/G1 arrest and cytostatic effect (Sathe et al., 2015). The correlation of therapy response and down-regulation of RB protein level has also been shown in a variety of tumors pre-clinically by other groups (Barton et al., 2013; Dean et al., 2010; Franco et al., 2014; Konecny et al., 2011; F. Liu & Korc, 2012; Miller et al., 2011; Sathe et al., 2015; von Witzleben et al., 2015; Witkiewicz et al., 2015). On the other hand, presence of RB1 is a pre-requisite for therapy response and RB1 negative cells are non-responsive to treatment (Comstock et al., 2013; Fry et al., 2004; Konecny et al., 2011; Michaud et al., 2010; Sathe et al., 2015; von Witzleben et al., 2015; Young et al., 2014). This observation seemingly is a contradiction between the reduction of RB1 upon CDK4/6 inhibition and the requirement of its expression for therapy response. A better understanding of mechanisms responsible for RB1 down-regulation upon CDK4/6 inhibition might be useful for understanding response mechanisms and might reveal predictive marker.

5.2 Expression of RB1 is necessary for therapy response

Pre-clinical studies have demonstrated that only tumor cell lines with expression of functional RB1 displayed sensitivity to CDK4/6 inhibition (Comstock et al., 2013; Fry et al., 2004; Konecny et al., 2011; Michaud et al., 2010; Sathe et al., 2015; von Witzleben et al., 2015; Young et al., 2014). In addition, original responsive cells, under the selection of prolonged treatment with CDK4/6 inhibitors, finally acquired a loss of RB1 and developed into resistant cells (Herrera-Abreu et al., 2016; Witkiewicz et al., 2015).

However, very few studies have evaluated the dependence on RB1 for therapy response in tumor cells with knockdown of RB1 expression and have shown contradictory findings. In this work, we show that RB1 positive cells gained resistance to CDK4/6 inhibition after siRNA-mediated silencing of RB1 expression (Bollard et al., 2016; Michaud et al., 2010; Zhang et al., 2014) as expected. However, such resistance was not clearly observed in breast cancer and hepatoma cells after knockdown of RB1 (Dean et al., 2010; Rivadeneira et al., 2010), which raised the option that the presence of RB1 is not universally required for therapy response under all circumstances. The observation that upon CDK4/6 inhibition a robust reduction of RB1 protein occurs might question its role in mediating therapy response. However, in our experiments T24 cells with knockdown of RB1 expression were no longer sensitive to CDK4/6 inhibitors. So our result further confirms the general view that the expression of RB1 is a prerequisite for therapy response to CDK4/6 inhibition.

5.3 Proteasomal degradation on RB1

Transcriptional repression and proteasome dependent protein degradation are potential mechanisms of how RB1 is down-regulated upon CDK4/6 inhibition.
Generally, proteins with a poly-ubiquitination formed on lysine 48 (K48) are recognized and degraded by the 26S proteasome, consisting of one 20S core particle and two 19S regulatory particles. This huge protein complex has a size of more than 2000 kDa and exists throughout the nucleus and cytoplasm of all eukaryotic cells (Adams, 2003; Lub et al., 2015).

We evaluated in detail the role of proteasome dependent degradation in RB1 down-regulation upon CDK4/6 inhibition. Several methods were applied for the manipulation of the proteasome dependent pathway. Apart from MG-132 which is a non specific proteasome inhibitor, another highly selective inhibitor, epoxomicin, was tested in combination with PD-0332991 and was observed to partially rescue the reduction of RB1, indicating a proteasome-mediated degradation. However, a deficiency of poly-ubiquitination on K48 that was achieved by overexpressing ubiquitin with K48 mutated (Uchida et al., 2005; Y. Wang et al., 2015), had no much effect on protecting RB1 from degradation upon CDK4/6 inhibition, which could be explained by either that this degradation is ubiquitin independent but proteasome dependent or that the amount of recombinant defective ubiquitin was insufficient to competitively inhibit activity of wild type ubiquitin. This has also been examined by one group which revealed a coordinate negative regulation of transcription and protein stability upon PD-0332991 treatment. However, the underlying mechanisms still remained elusive (Yoshida et al., 2016).

Several viral oncoproteins, such as Human Papillomavirus (HPV) E7 (Boyer, Wazer, & Band, 1996) and human cytomegalovirus (CMV) pp71 (Kalejta, Bechtel, & Shenk, 2003), and three cellular oncoproteins, including MDM2 (Sdek et al., 2005; Uchida et al., 2005; Ying & Xiao, 2006), gankyrin (Higashitsuji et al., 2000) and NRBE3 (Y. Wang et al., 2015), have been reported to associate with specific domains of RB1 and promote its degradation via the ubiquitin-proteasome pathway. Among them, MDM2 is the most widely studied, with an identification of its binding in the C-terminus of RB1 (Xiao et al., 1995; Ying & Xiao, 2006), and is able to destabilize RB1 in either ubiquitin dependent or ubiquitin independent proteasome pathways. In our present study, we repressed the expression of MDM2 which is required for proteasomal degradation of RB1 upon CDK4/6 inhibition. Then the physical connection of MDM2 to RB1 was manipulated by cloning a recombinant C-terminus-deleted RB1 (RB1-C42) in order to examine the dependence of RB1 degradation on MDM2 upon CDK4/6 inhibition. On the other hand, another recombinant RB1 with all phosphorylation sites mutated (RB1-CDK) was used to examine whether dephosphorylation on RB1 contributes to its degradation in response to CDK4/6 inhibition. Several unique aspects of RB1 degradation in response to CDK4/6 inhibition have been shown. First, MDM2 binding to the C-terminus of RB1 are

required for proteasomal degradation of RB1 upon CDK4/6 inhibition. Second, de-phosphorylation on RB1 from CDK4/6 inhibition is not a prerequisite for MDM2-dependent RB1 degradation. This is not consistent with the known mechanism that MDM2 selectively binds to hypophosphorylated RB1 and promotes further degradation (Sdek et al., 2004). So, instead of suppression on RB1 phosphorylation, other unknown downstream targets of CDK4/6 that might be responsible for regulating proteolytic activity of MDM2 on RB1 could be potential promoters for the degradation of RB1 upon CDK4/6 inhibition. . . However, the resistance of RB1-C42 to degradation was only observed in RT112 cells, but not in T24. This inconsistency could be explained by variation of molecular landscape among different cell lines. For example, in T24, the MDM2 binding site might not locate in the C-terminus of RB1. Or MDM2 mediated the degradation of RB1 through an indirect interaction. A last explanation might be also an MDM2 independent targeting of RB1 for degradation. The experiments have to be extended among other BC cell lines to comfirm whether this observation is exclusive or universal.

Our observation that synchronous reduction of total RB1 and phosphorylated RB1 was correlated with cell cycle arrest upon CDK4/6 inhibition has also been reported by other groups (Dean et al., 2010; Konecny et al., 2011; Rader et al., 2013). They attributed the cell cycle arrest to suppression of RB1 phosphorylation, while the implication of RB1 down-regualtion in therapy response is poorly discussed. We evaluated how therapy response could be influenced via down-regulation of total RB1. And we observed that the stabilization of RB1 via knockdown of MDM2 interfered with the initial therapy response in a time-dependent manner. However, this interference with therapy response was unable to be observed under prolonged CDK4/6 inhibition at 24 hour, which can be explained by that the therapy response to CDK4/6 inhibition is only partially via MDM2-mediated degradation on RB1. And other biochemical effects in response to the treatment, such as a suppression on RB1 transcription, might also contribute to the therapy response. Our current data at least demonstrate that the down-regulation of not only RB1 phosphorylation but also its total protein level are indicators of therapy response during the treatment with CDK4/6 inhibitors.

5.3 Partial recovery of cell cycle progression under prolonged CDK4/6 inhibition

Though a robust cell cycle arrest was induced upon acute CDK4/6 inhibition for 24 hours, a proportion of quiescent cells were restored to cell cycle progression under prolonged treatment for over 48 hours, accompanied by a partial recurrence of RB1 phosphorylation and downstreams of E2Fs, like cyclin E2 and E2F1. This observation was consistent with our results from cell viability assay that cytoproliferation under prolonged treatment was merely restricted at a lower speed, but was never completely terminated. Similar adaptive therapy resistance developed under prolonged CDK4/6 inhibition was also reported and attributed to compensative activation of CDK2-RB1 pathway probably via its decreased interaction with p27 (L. Wang et al., 2007) or increased interaction with cyclin D1 (Herrera-Abreu et al., 2016). This mechanism might be also functional in our model in which the additional CDK2 inhibition by roscovitine prevented the reentry into cell cycle under the prolonged single CDK4/6 inhibition, accompanied by a repression of RB1 and phosphorylated RB1, cyclin D1, E2 and E2F1. In absence of CDK4/6 inhibition, regular cell cycle progression predominantly relies on activation of CDK4/6 instead of that of CDK2. This has been supported by the observation that either treating with CDK2 inhibitors in our BC models or knocking down CDK2 expression in breast cancer (Herrera-Abreu et al., 2016) had minimal effect on cell cycle and phosphorylation of RB1. These observations indicate that CDK4/6-activated phosphorylation on RB1 is sufficient to promote G1/S transition, and the subsequent CDK2-activated phosphorylation on RB1 is not indispensable. However, under the circumstances that cell cycle regulation no longer depends on CDK4/6 due to loss of CDK4/6 (Malumbres et al., 2004) or that CDK4/6 activity is inhibited artificially by specific inhibitors, the functional CDK2 might replace the role of CDK4/6 in phosphorylating RB1 and mediates G1/S transition, while CDK2 inhibition is able to prevent recurrent phosphorylation on RB1. Also, single-cell analysis of CDK2 activity showed a higher level of CDK2 activity in PD-0332991 resistant breast cancer cells compared to PD-0332991 sensitive ones (U. S. Asghar et al., 2017). As far as the current recommended course of CDK4/6 inhibitors is concerned (Cristofanilli et al., 2016; Hortobagyi et al., 2016), RB1 positive tumor cells would have high opportunities to escape absolute cell cycle arrest during the 21 days of therapy.

Therefore, it is rational to apply potential combinative therapies to completely inhibit the activation of pathways involved in cell cycle progression.

5.4 The role of E2Fs in CDK4/6-RB1 pathway and therapy response

In our model of BC, we provided an overview on the kinetics of E2F1-5 upon CDK4/6 inhibition and found that the expression of E2F1-5 were differentially modulated. Interestingly, the expression of E2F1 is down-regulated immediately followed by a partial recovery during 3 days of CDK4/6 inhibition, which highly correlates with the observed cell cycle reentry and re-phosphorylation on RB1. As far as the correlation was concerned, we supposed that a thorough and stable suppression of the activity and expression of E2F1 was required for therapy response and overcoming adaptive therapy resistance under prolonged treatment. However, whether in absence or presence of CDK4/6 inhibitors, the depletion of E2F1by siRNA had no effect on cell cycle progression, indicating that E2F1 alone is not required for cell cycle progression in our model. Our observation that E2F2 and -3 are rather up-regulated 24 hours after treatment does not support a redundant function that could substitute loss of E2F1. The underlying function of E2F family in cell cycle progression and its role in therapy response to CDK4/6 inhibition remains further study.

E2F1-3, apart from some overlapping functions, have their individual functions and regulations on their unique target genes. It has been reported that induction of apoptosis is an exclusive function of E2F1 via its specifically binding to and repressing the Mcl-1 promoter (Croxton, Ma, Song, Haura, & Cress, 2002; Hallstrom & Nevins, 2003). In contrast, Schlisio et al has demonstrated that not E2F1 but E2F2 and E2F3, with association to YY1 and RYBP, bound to the Cdc6 promoter and activated its transcription, which is necessary for an intact G1/S transition (Schlisio, Halperin, Vidal, & Nevins, 2002). Preclinical studies in vitro have shown that overexpression of E2F2 in PD-0332991 sensitive breast cancer and hepatoma cells caused therapy resistance (Dean et al., 2010; Rivadeneira et al., 2010). Other connections between E2Fs and therapy response to CDK4/6 inhibition are poorly evaluated. So the differential implications of these E2Fs for therapy response remain further study in our model of BC.

Drosophila genome encodes only a unique activating E2F gene, dE2F1, and its activity and expression determines the fate of cell cycle progression. Overexpression

of dE2F1 induced an increased S phase entry (Du, Xie, & Dyson, 1996), while dysfunctional mutation (Frolov et al., 2001) or depletion by siRNA of dE2F1 (Frolov et al., 2003) resulted in a G1 phase arrest, which indicated that, in this case, E2F1 played an indispensable role in G1/S transition. However, mammalian genome encodes three different activating E2Fs, which makes this regulation more complicated and adaptive. Upon loss of only one activating E2F, its function might be compensated and substituted by other E2Fs, as observed in mouse embryonic fibroblasts. Also, only a combined loss of E2F1-3 factors can thoroughly repressed expression of E2F target genes and impeded G1/S transition (Wu et al., 2001).

6. Summary

Cisplatin-based chemotherapy has been deployed as the first-line therapy for advanced bladder cancer for over 30 years. However, even after the chemotherapy, the disease specific survival of patients with regional lymph node invasion or distant metastasis is still quite poor. Target therapy, which is designed to selectively inhibit the cellular molecular pathways necessary for cancer viability and progression, has been deployed as a novel therapeutic strategy in a wide range of cancer since 1990s. Unfortunately, though targeting the immune checkpoint could be a promising therapy in a small ratio of advanced BCs, so far no other target therapy has been approved by FDA or evaluated in phase III clinical trial for BC therapy.

The CDK4/6-RB1-E2F pathway, which regulates the transition of cell cycle from G1 phase to S phase, is frequently disrupted in 93% of advanced bladder cancer. Our previous work has characterized the CDK4/6-RB1 pathway as a potential therapy target in BC testing the effects of CDK4/6 inhibitors in vitro and in vivo. In this project, we further studied molecular mechanisms induced by CDK4/6 inhibitor PD-0332991 and analyzed the roles of these molecules in therapy response.

A prerequisite for response to CDK4/6 inhibitors was the expression of RB1, since RB1-negative cells, which were either RB1 mutant or established via RB1 knockdown, were resistant to CDK4/6 inhibition. We also observed that the therapy response of RB1-positive cell lines, T24 and RT112, to PD-0332991 correlated with a synchronous robust reduction in protein level of both total and phosphorylated RB1. The mechanism underlying the down-regulation on RB1 upon CDK4/6 inhibition was characterized next. First, we revealed a transcriptional repression on RB1 upon the treatment by RT-qPCR. Second, we observed that proteasome inhibition partially rescue the down-regulation of RB1, indicating a proteasomal degradation of RB1 upon the treatment. MDM2 was identified as a mediator that promoted the proteasomal degradation of RB1 upon CDK4/6 inhibition. Silencing of MDM2 by siRNA interfered with the degradation on RB1 and the therapy response in a time-dependent manner. Furthermore, recombinant HA-tagged wild type RB1 (RB1-WT), mutant RB1 lacking the C-terminal 42 amino acids (RB1-C42) and mutant RB1 with all CDKs phosphorylation sites mutated (RB1-CDK) were introduced into BC cells to compare their stability in response to PD-0332991. We observed that the de-

phosphorylation of RB1 is not a prerequisite for its further degradation. But the MDM2-binding to RB1 is required for its degradation upon CDK4/6 inhibition. Besides, analysis on the functional and biochemical effects of prolonged CDK4/6 inhibition revealed a partial recovery of cell cycle progression and re-phosphorylation of RB1.The effects were also accompanied by a precise differential regulation on protein levels of E2F family.

Overall, this work on molecular mechanisms induced by CDK4/6 inhibition raised a contradiction between two opposite observations. Therapy response correlated with a decrease of RB1, while the expression of RB1 is required for therapy response, indicating that the role of RB1 in CDK4/6 inhibition is complicated and still not thoroughly interpreted. This complexity is also consistent with the fact that RB1 is not a reliable biomarker to predict therapy response in clinical trials. Both transcriptional repression and MDM2-dependent proteasomal degradation are involved in this down-regulation of RB1 upon CDK4/6 inhibition. In addition, a partial adaptive resistance to prolonged treatment with mono-CDK4/6 inhibition is another challenge for therapy.

Bibliography

Abraham, R. T. (2001). Cell cycle checkpoint signaling through the ATM and ATR kinases. *Genes Dev, 15*(17), 2177-2196. doi:10.1101/gad.914401

Acevedo, M., Vernier, M., Mignacca, L., Lessard, F., Huot, G., Moiseeva, O., Bourdeau, V., & Ferbeyre, G. (2016a). A CDK4/6-Dependent Epigenetic Mechanism Protects Cancer Cells from PML-induced Senescence. *Cancer Res*. doi:10.1158/0008-5472.can-15-2347

Acevedo, M., Vernier, M., Mignacca, L., Lessard, F., Huot, G., Moiseeva, O., Bourdeau, V., & Ferbeyre, G. (2016b). A CDK4/6-Dependent Epigenetic Mechanism Protects Cancer Cells from PML-induced Senescence. *Cancer Res, 76*(11), 3252-3264. doi:10.1158/0008-5472.can-15-2347

Adams, J. (2003). The proteasome: structure, function, and role in the cell. *Cancer Treat Rev, 29 Suppl 1*, 3-9.

Asghar, U., Witkiewicz, A. K., Turner, N. C., & Knudsen, E. S. (2015). The history and future of targeting cyclin-dependent kinases in cancer therapy. *Nat Rev Drug Discov, 14*(2), 130-146. doi:10.1038/nrd4504

Asghar, U. S., Barr, A. R., Cutts, R., Beaney, M., Babina, I., Sampath, D., Giltnane, J., Lacap, J. A., Crocker, L., Young, A., Pearson, A., Herrera-Abreu, M. T., Bakal, C., & Turner, N. C. (2017). Single-Cell Dynamics Determines Response to CDK4/6 Inhibition in Triple-Negative Breast Cancer. *Clin Cancer Res, 23*(18), 5561-5572. doi:10.1158/1078-0432.ccr-17-0369

Barton, K. L., Misuraca, K., Cordero, F., Dobrikova, E., Min, H. D., Gromeier, M., Kirsch, D. G., & Becher, O. J. (2013). PD-0332991, a CDK4/6 inhibitor, significantly prolongs survival in a genetically engineered mouse model of brainstem glioma. *PLoS One, 8*(10), e77639. doi:10.1371/journal.pone.0077639

Benzeno, S., Lu, F., Guo, M., Barbash, O., Zhang, F., Herman, J. G., Klein, P. S., Rustgi, A., & Diehl, J. A. (2006). Identification of mutations that disrupt phosphorylation-dependent nuclear export of cyclin D1. *Oncogene, 25*(47), 6291-6303. doi:10.1038/sj.onc.1209644

Bernardes de Jesus, B., & Blasco, M. A. (2012). Assessing cell and organ senescence biomarkers. *Circ Res, 111*(1), 97-109. doi:10.1161/circresaha.111.247866

Bollard, J., Miguela, V., Ruiz de Galarreta, M., Venkatesh, A., Bian, C. B., Roberto, M. P., Tovar, V., Sia, D., Molina-Sanchez, P., Nguyen, C. B., Nakagawa, S., Llovet, J. M., Hoshida, Y., & Lujambio, A. (2016). Palbociclib (PD-0332991), a selective CDK4/6 inhibitor, restricts tumour growth in preclinical models of hepatocellular carcinoma. *Gut*. doi:10.1136/gutjnl-2016-312268

Bourdeau, V., & Ferbeyre, G. (2016). CDK4-CDK6 inhibitors induce autophagy-mediated degradation of DNMT1 and facilitate the senescence antitumor response. *Autophagy, 12*(10), 1965-1966. doi:10.1080/15548627.2016.1214779

Boyer, S. N., Wazer, D. E., & Band, V. (1996). E7 protein of human papilloma virus-16 induces degradation of retinoblastoma protein through the ubiquitin-proteasome pathway. *Cancer Res, 56*(20), 4620-4624.

Buckley, M. F., Sweeney, K. J., Hamilton, J. A., Sini, R. L., Manning, D. L., Nicholson, R. I., deFazio, A., Watts, C. K., Musgrove, E. A., & Sutherland, R. L. (1993). Expression and amplification of cyclin genes in human breast cancer. *Oncogene, 8*(8), 2127-2133.

Burger, M., Catto, J. W., Dalbagni, G., Grossman, H. B., Herr, H., Karakiewicz, P., Kassouf, W., Kiemeney, L. A., La Vecchia, C., Shariat, S., & Lotan, Y. (2013). Epidemiology and risk factors of urothelial bladder cancer. *Eur Urol, 63*(2), 234-241.

doi:10.1016/j.eururo.2012.07.033
Burkhart, D. L., Ngai, L. K., Roake, C. M., Viatour, P., Thangavel, C., Ho, V. M., Knudsen, E. S., & Sage, J. (2010). Regulation of RB transcription in vivo by RB family members. *Mol Cell Biol, 30*(7), 1729-1745. doi:10.1128/mcb.00952-09
Campisi, J., & d'Adda di Fagagna, F. (2007). Cellular senescence: when bad things happen to good cells. *Nat Rev Mol Cell Biol, 8*(9), 729-740. doi:10.1038/nrm2233
Carneiro, B. A., Meeks, J. J., Kuzel, T. M., Scaranti, M., Abdulkadir, S. A., & Giles, F. J. (2015). Emerging therapeutic targets in bladder cancer. *Cancer Treat Rev, 41*(2), 170-178. doi:10.1016/j.ctrv.2014.11.003
Chavan, S., Bray, F., Lortet-Tieulent, J., Goodman, M., & Jemal, A. (2014). International variations in bladder cancer incidence and mortality. *Eur Urol, 66*(1), 59-73. doi:10.1016/j.eururo.2013.10.001
Cheng, S., Andrew, A. S., Andrews, P. C., & Moore, J. H. (2016). Complex systems analysis of bladder cancer susceptibility reveals a role for decarboxylase activity in two genome-wide association studies. *BioData Min, 9*, 40. doi:10.1186/s13040-016-0119-z
Collado, M., Gil, J., Efeyan, A., Guerra, C., Schuhmacher, A. J., Barradas, M., Benguria, A., Zaballos, A., Flores, J. M., Barbacid, M., Beach, D., & Serrano, M. (2005). Tumour biology: senescence in premalignant tumours. *Nature, 436*(7051), 642. doi:10.1038/436642a
Collado, M., & Serrano, M. (2010). Senescence in tumours: evidence from mice and humans. *Nat Rev Cancer, 10*(1), 51-57. doi:10.1038/nrc2772
Colt, J. S., Friesen, M. C., Stewart, P. A., Donguk, P., Johnson, A., Schwenn, M., Karagas, M. R., Armenti, K., Waddell, R., Verrill, C., Ward, M. H., Freeman, L. E., Moore, L. E., Koutros, S., Baris, D., & Silverman, D. T. (2014). A case-control study of occupational exposure to metalworking fluids and bladder cancer risk among men. *Occup Environ Med, 71*(10), 667-674. doi:10.1136/oemed-2013-102056
Comstock, C. E., Augello, M. A., Goodwin, J. F., de Leeuw, R., Schiewer, M. J., Ostrander, W. F., Jr., Burkhart, R. A., McClendon, A. K., McCue, P. A., Trabulsi, E. J., Lallas, C. D., Gomella, L. G., Centenera, M. M., Brody, J. R., Butler, L. M., Tilley, W. D., & Knudsen, K. E. (2013). Targeting cell cycle and hormone receptor pathways in cancer. *Oncogene, 32*(48), 5481-5491. doi:10.1038/onc.2013.83
Cristofanilli, M., Turner, N. C., Bondarenko, I., Ro, J., Im, S. A., Masuda, N., Colleoni, M., DeMichele, A., Loi, S., Verma, S., Iwata, H., Harbeck, N., Zhang, K., Theall, K. P., Jiang, Y., Bartlett, C. H., Koehler, M., & Slamon, D. (2016). Fulvestrant plus palbociclib versus fulvestrant plus placebo for treatment of hormone-receptor-positive, HER2-negative metastatic breast cancer that progressed on previous endocrine therapy (PALOMA-3): final analysis of the multicentre, double-blind, phase 3 randomised controlled trial. *Lancet Oncol, 17*(4), 425-439. doi:10.1016/s1470-2045(15)00613-0
Croxton, R., Ma, Y., Song, L., Haura, E. B., & Cress, W. D. (2002). Direct repression of the Mcl-1 promoter by E2F1. *Oncogene, 21*(9), 1359-1369. doi:10.1038/sj.onc.1205157
Dean, J. L., McClendon, A. K., Hickey, T. E., Butler, L. M., Tilley, W. D., Witkiewicz, A. K., & Knudsen, E. S. (2012). Therapeutic response to CDK4/6 inhibition in breast cancer defined by ex vivo analyses of human tumors. *Cell Cycle, 11*(14), 2756-2761. doi:10.4161/cc.21195
Dean, J. L., Thangavel, C., McClendon, A. K., Reed, C. A., & Knudsen, E. S. (2010). Therapeutic CDK4/6 inhibition in breast cancer: key mechanisms of response and failure. *Oncogene, 29*(28), 4018-4032. doi:10.1038/onc.2010.154

Debacq-Chainiaux, F., Erusalimsky, J. D., Campisi, J., & Toussaint, O. (2009). Protocols to detect senescence-associated beta-galactosidase (SA-betagal) activity, a biomarker of senescent cells in culture and in vivo. *Nat Protoc, 4*(12), 1798-1806. doi:10.1038/nprot.2009.191

DeMichele, A., Clark, A. S., Tan, K. S., Heitjan, D. F., Gramlich, K., Gallagher, M., Lal, P., Feldman, M., Zhang, P., Colameco, C., Lewis, D., Langer, M., Goodman, N., Domchek, S., Gogineni, K., Rosen, M., Fox, K., & O'Dwyer, P. (2015). CDK 4/6 inhibitor palbociclib (PD0332991) in Rb+ advanced breast cancer: phase II activity, safety, and predictive biomarker assessment. *Clin Cancer Res, 21*(5), 995-1001. doi:10.1158/1078-0432.CCR-14-2258

Dickson, M. A. (2014). Molecular pathways: CDK4 inhibitors for cancer therapy. *Clin Cancer Res, 20*(13), 3379-3383. doi:10.1158/1078-0432.ccr-13-1551

Divakar, S. K., Ramana Reddy, M. V., Cosenza, S. C., Baker, S. J., Perumal, D., Antonelli, A. C., Brody, J., Akula, B., Parekh, S., & Premkumar Reddy, E. (2015). Dual inhibition of CDK4/Rb and PI3K/AKT/mTOR pathways by ON123300 induces synthetic lethality in mantle cell lymphomas. *Leukemia*. doi:10.1038/leu.2015.185

Du, W., Xie, J. E., & Dyson, N. (1996). Ectopic expression of dE2F and dDP induces cell proliferation and death in the Drosophila eye. *Embo Journal, 15*(14), 3684-3692.

Egbers, L., Grotenhuis, A. J., Aben, K. K., Alfred Witjes, J., Kiemeney, L. A., & Vermeulen, S. H. (2015). The prognostic value of family history among patients with urinary bladder cancer. *Int J Cancer, 136*(5), 1117-1124. doi:10.1002/ijc.29062

el-Deiry, W. S., Tokino, T., Velculescu, V. E., Levy, D. B., Parsons, R., Trent, J. M., Lin, D., Mercer, W. E., Kinzler, K. W., & Vogelstein, B. (1993). WAF1, a potential mediator of p53 tumor suppression. *Cell, 75*(4), 817-825.

Finn, R. S., Crown, J. P., Lang, I., Boer, K., Bondarenko, I. M., Kulyk, S. O., Ettl, J., Patel, R., Pinter, T., Schmidt, M., Shparyk, Y., Thummala, A. R., Voytko, N. L., Fowst, C., Huang, X., Kim, S. T., Randolph, S., & Slamon, D. J. (2015). The cyclin-dependent kinase 4/6 inhibitor palbociclib in combination with letrozole versus letrozole alone as first-line treatment of oestrogen receptor-positive, HER2-negative, advanced breast cancer (PALOMA-1/TRIO-18): a randomised phase 2 study. *Lancet Oncol, 16*(1), 25-35. doi:10.1016/S1470-2045(14)71159-3

Finn, R. S., Dering, J., Conklin, D., Kalous, O., Cohen, D. J., Desai, A. J., Ginther, C., Atefi, M., Chen, I., Fowst, C., Los, G., & Slamon, D. J. (2009). PD 0332991, a selective cyclin D kinase 4/6 inhibitor, preferentially inhibits proliferation of luminal estrogen receptor-positive human breast cancer cell lines in vitro. *Breast Cancer Res, 11*(5), R77. doi:10.1186/bcr2419

Franco, J., Balaji, U., Freinkman, E., Witkiewicz, A. K., & Knudsen, E. S. (2016). Metabolic Reprogramming of Pancreatic Cancer Mediated by CDK4/6 Inhibition Elicits Unique Vulnerabilities. *Cell Rep, 14*(5), 979-990. doi:10.1016/j.celrep.2015.12.094

Franco, J., Witkiewicz, A. K., & Knudsen, E. S. (2014). CDK4/6 inhibitors have potent activity in combination with pathway selective therapeutic agents in models of pancreatic cancer. *Oncotarget, 5*(15), 6512-6525.

Frolov, M. V., Huen, D. S., Stevaux, O., Dimova, D., Balczarek-Strang, K., Elsdon, M., & Dyson, N. J. (2001). Functional antagonism between E2F family members. *Genes & Development, 15*(16), 2146.

Frolov, M. V., Stevaux, O., Moon, N. S., Dimova, D., Kwon, E. J., Morris, E. J., & Dyson, N. J. (2003). G1 cyclin-dependent kinases are insufficient to reverse dE2F2-mediated repression. *Genes Dev, 17*(6), 723-728. doi:10.1101/gad.1031803

Fry, D. W., Harvey, P. J., Keller, P. R., Elliott, W. L., Meade, M., Trachet, E., Albassam, M.,

Zheng, X., Leopold, W. R., Pryer, N. K., & Toogood, P. L. (2004). Specific inhibition of cyclin-dependent kinase 4/6 by PD 0332991 and associated antitumor activity in human tumor xenografts. *Mol Cancer Ther, 3*(11), 1427-1438.

Garcia-Closas, M., Ye, Y., Rothman, N., Figueroa, J. D., Malats, N., Dinney, C. P., Chatterjee, N., Prokunina-Olsson, L., Wang, Z., Lin, J., Real, F. X., Jacobs, K. B., Baris, D., Thun, M., De Vivo, I., Albanes, D., Purdue, M. P., Kogevinas, M., Kamat, A. M., Lerner, S. P., Grossman, H. B., Gu, J., Pu, X., Hutchinson, A., Fu, Y. P., Burdett, L., Yeager, M., Tang, W., Tardon, A., Serra, C., Carrato, A., Garcia-Closas, R., Lloreta, J., Johnson, A., Schwenn, M., Karagas, M. R., Schned, A., Andriole, G., Jr., Grubb, R., 3rd, Black, A., Jacobs, E. J., Diver, W. R., Gapstur, S. M., Weinstein, S. J., Virtamo, J., Hunter, D. J., Caporaso, N., Landi, M. T., Fraumeni, J. F., Jr., Silverman, D. T., Chanock, S. J., & Wu, X. (2011). A genome-wide association study of bladder cancer identifies a new susceptibility locus within SLC14A1, a urea transporter gene on chromosome 18q12.3. *Hum Mol Genet, 20*(21), 4282-4289. doi:10.1093/hmg/ddr342

Ghosh, M., Brancato, S. J., Agarwal, P. K., & Apolo, A. B. (2014). Targeted therapies in urothelial carcinoma. *Curr Opin Oncol, 26*(3), 305-320. doi:10.1097/cco.0000000000000064

Giacinti, C., & Giordano, A. (2006). RB and cell cycle progression. *Oncogene, 25*(38), 5220-5227. doi:10.1038/sj.onc.1209615

Gill, R. M., Hamel, P. A., Zhe, J., Zacksenhaus, E., Gallie, B. L., & Phillips, R. A. (1994). Characterization of the human RB1 promoter and of elements involved in transcriptional regulation. *Cell Growth Differ, 5*(5), 467-474.

Hallstrom, T. C., & Nevins, J. R. (2003). Specificity in the activation and control of transcription factor E2F-dependent apoptosis. *Proc Natl Acad Sci U S A, 100*(19), 10848-10853. doi:10.1073/pnas.1831408100

Hamel, P. A., Gill, R. M., Phillips, R. A., & Gallie, B. L. (1992). Transcriptional repression of the E2-containing promoters EIIaE, c-myc, and RB1 by the product of the RB1 gene. *Mol Cell Biol, 12*(8), 3431-3438.

Hart, L. S., Rader, J., Raman, P., Batra, V., Russell, M. R., Tsang, M., Gagliardi, M., Chen, L., Martinez, D., Li, Y., Wood, A., Kim, S., Parasuraman, S., Delach, S., Cole, K. A., Krupa, S., Boehm, M., Peters, M., Caponigro, G., & Maris, J. M. (2016). Preclinical therapeutic synergy of MEK1/2 and CDK4/6 inhibition in neuroblastoma. *Clin Cancer Res*. doi:10.1158/1078-0432.ccr-16-1131

Hayflick, L., & Koprowski, H. (1965). DIRECT AGAR ISOLATION OF MYCOPLASMAS FROM HUMAN LEUKAEMIC BONE MARROW. *Nature, 205*, 713-714.

Heilmann, A. M., Perera, R. M., Ecker, V., Nicolay, B. N., Bardeesy, N., Benes, C. H., & Dyson, N. J. (2014). CDK4/6 and IGF1 receptor inhibitors synergize to suppress the growth of p16INK4A-deficient pancreatic cancers. *Cancer Res, 74*(14), 3947-3958. doi:10.1158/0008-5472.can-13-2923

Herrera-Abreu, M. T., Palafox, M., Asghar, U., Rivas, M. A., Cutts, R. J., Garcia-Murillas, I., Pearson, A., Guzman, M., Rodriguez, O., Grueso, J., Bellet, M., Cortes, J., Elliott, R., Pancholi, S., Baselga, J., Dowsett, M., Martin, L. A., Turner, N. C., & Serra, V. (2016). Early Adaptation and Acquired Resistance to CDK4/6 Inhibition in Estrogen Receptor-Positive Breast Cancer. *Cancer Res, 76*(8), 2301-2313. doi:10.1158/0008-5472.can-15-0728

Higashitsuji, H., Itoh, K., Nagao, T., Dawson, S., Nonoguchi, K., Kido, T., Mayer, R. J., Arii, S., & Fujita, J. (2000). Reduced stability of retinoblastoma protein by gankyrin, an oncogenic ankyrin-repeat protein overexpressed in hepatomas. *Nat Med, 6*(1), 96-99. doi:10.1038/71600

Hortobagyi, G. N., Stemmer, S. M., Burris, H. A., Yap, Y. S., Sonke, G. S., Paluch-Shimon, S.,

Campone, M., Blackwell, K. L., Andre, F., Winer, E. P., Janni, W., Verma, S., Conte, P., Arteaga, C. L., Cameron, D. A., Petrakova, K., Hart, L. L., Villanueva, C., Chan, A., Jakobsen, E., Nusch, A., Burdaeva, O., Grischke, E. M., Alba, E., Wist, E., Marschner, N., Favret, A. M., Yardley, D., Bachelot, T., Tseng, L. M., Blau, S., Xuan, F., Souami, F., Miller, M., Germa, C., Hirawat, S., & O'Shaughnessy, J. (2016). Ribociclib as First-Line Therapy for HR-Positive, Advanced Breast Cancer. *N Engl J Med, 375*(18), 1738-1748. doi:10.1056/NEJMoa1609709

Humphrey, P. A., Moch, H., Cubilla, A. L., Ulbright, T. M., & Reuter, V. E. (2016). The 2016 WHO Classification of Tumours of the Urinary System and Male Genital Organs-Part B: Prostate and Bladder Tumours. *Eur Urol, 70*(1), 106-119. doi:10.1016/j.eururo.2016.02.028

Infante, J. R., Cassier, P. A., Gerecitano, J. F., Witteveen, P. O., Chugh, R., Ribrag, V., Chakraborty, A., Matano, A., Dobson, J. R., Crystal, A. S., Parasuraman, S., & Shapiro, G. I. (2016). A Phase I Study of the Cyclin-Dependent Kinase 4/6 Inhibitor Ribociclib (LEE011) in Patients with Advanced Solid Tumors and Lymphomas. *Clin Cancer Res, 22*(23), 5696-5705. doi:10.1158/1078-0432.CCR-16-1248

Janicke, R. U., Walker, P. A., Lin, X. Y., & Porter, A. G. (1996). Specific cleavage of the retinoblastoma protein by an ICE-like protease in apoptosis. *EMBO J, 15*(24), 6969-6978.

Jiang, W., Kahn, S. M., Tomita, N., Zhang, Y. J., Lu, S. H., & Weinstein, I. B. (1992). Amplification and expression of the human cyclin D gene in esophageal cancer. *Cancer Res, 52*(10), 2980-2983.

Kalejta, R. F., Bechtel, J. T., & Shenk, T. (2003). Human cytomegalovirus pp71 stimulates cell cycle progression by inducing the proteasome-dependent degradation of the retinoblastoma family of tumor suppressors. *Mol Cell Biol, 23*(6), 1885-1895.

Kennedy, A. L., Vallurupalli, M., Chen, L., Crompton, B., Cowley, G., Vazquez, F., Weir, B. A., Tsherniak, A., Parasuraman, S., Kim, S., Alexe, G., & Stegmaier, K. (2015). Functional, chemical genomic, and super-enhancer screening identify sensitivity to cyclin D1/CDK4 pathway inhibition in Ewing sarcoma. *Oncotarget*.

Khatib, Z. A., Matsushime, H., Valentine, M., Shapiro, D. N., Sherr, C. J., & Look, A. T. (1993). Coamplification of the CDK4 gene with MDM2 and GLI in human sarcomas. *Cancer Res, 53*(22), 5535-5541.

Knudsen, E. S., & Knudsen, K. E. (2008). Tailoring to RB: tumour suppressor status and therapeutic response. *Nat Rev Cancer, 8*(9), 714-724. doi:10.1038/nrc2401

Knudsen, E. S., & Witkiewicz, A. K. (2016). Defining the transcriptional and biological response to CDK4/6 inhibition in relation to ER+/HER2- breast cancer. *Oncotarget*. doi:10.18632/oncotarget.11588

Konecny, G. E., Winterhoff, B., Kolarova, T., Qi, J., Manivong, K., Dering, J., Yang, G., Chalukya, M., Wang, H. J., Anderson, L., Kalli, K. R., Finn, R. S., Ginther, C., Jones, S., Velculescu, V. E., Riehle, D., Cliby, W. A., Randolph, S., Koehler, M., Hartmann, L. C., & Slamon, D. J. (2011). Expression of p16 and retinoblastoma determines response to CDK4/6 inhibition in ovarian cancer. *Clin Cancer Res, 17*(6), 1591-1602. doi:10.1158/1078-0432.ccr-10-2307

Kovatcheva, M., Liu, D. D., Dickson, M. A., Klein, M. E., O'Connor, R., Wilder, F. O., Socci, N. D., Tap, W. D., Schwartz, G. K., Singer, S., Crago, A. M., & Koff, A. (2015). MDM2 turnover and expression of ATRX determine the choice between quiescence and senescence in response to CDK4 inhibition. *Oncotarget, 6*(10), 8226-8243.

Kuilman, T., Michaloglou, C., Mooi, W. J., & Peeper, D. S. (2010). The essence of senescence. *Genes Dev, 24*(22), 2463-2479. doi:10.1101/gad.1971610

LaPak, K. M., & Burd, C. E. (2014). The molecular balancing act of p16(INK4a) in cancer

and aging. *Mol Cancer Res, 12*(2), 167-183. doi:10.1158/1541-7786.mcr-13-0350
Lee, M. S., Helms, T. L., Feng, N., Gay, J., Chang, Q. E., Tian, F., Wu, J. Y., Toniatti, C., Heffernan, T. P., Powis, G., Kwong, L. N., & Kopetz, S. (2016). Efficacy of the combination of MEK and CDK4/6 inhibitors in vitro and in vivo in KRAS mutant colorectal cancer models. *Oncotarget*. doi:10.18632/oncotarget.9153
Liggett, W. H., Jr., & Sidransky, D. (1998). Role of the p16 tumor suppressor gene in cancer. *J Clin Oncol, 16*(3), 1197-1206.
Lim, K. L., Chew, K. C., Tan, J. M., Wang, C., Chung, K. K., Zhang, Y., Tanaka, Y., Smith, W., Engelender, S., Ross, C. A., Dawson, V. L., & Dawson, T. M. (2005). Parkin mediates nonclassical, proteasomal-independent ubiquitination of synphilin-1: implications for Lewy body formation. *J Neurosci, 25*(8), 2002-2009. doi:10.1523/jneurosci.4474-04.2005
Lim, S., & Kaldis, P. (2013). Cdks, cyclins and CKIs: roles beyond cell cycle regulation. *Development, 140*(15), 3079-3093. doi:10.1242/dev.091744
Liu, F., & Korc, M. (2012). Cdk4/6 inhibition induces epithelial-mesenchymal transition and enhances invasiveness in pancreatic cancer cells. *Mol Cancer Ther, 11*(10), 2138-2148. doi:10.1158/1535-7163.mct-12-0562
Liu, H., Tang, X., Srivastava, A., Pecot, T., Daniel, P., Hemmelgarn, B., Reyes, S., Fackler, N., Bajwa, A., Kladney, R., Koivisto, C., Chen, Z., Wang, Q., Huang, K., Machiraju, R., Saenz-Robles, M. T., Cantalupo, P., Pipas, J. M., & Leone, G. (2015). Redeployment of Myc and E2f1-3 drives Rb-deficient cell cycles. *Nat Cell Biol, 17*(8), 1036-1048. doi:10.1038/ncb3210
Livak, K. J., & Schmittgen, T. D. (2001). Analysis of relative gene expression data using real-time quantitative PCR and the 2(-Delta Delta C(T)) Method. *Methods, 25*(4), 402-408. doi:10.1006/meth.2001.1262
Logan, J. E., Mostofizadeh, N., Desai, A. J., E, V. O. N. E., Conklin, D., Konkankit, V., Hamidi, H., Eckardt, M., Anderson, L., Chen, H. W., Ginther, C., Taschereau, E., Bui, P. H., Christensen, J. G., Belldegrun, A. S., Slamon, D. J., & Kabbinavar, F. F. (2013). PD-0332991, a potent and selective inhibitor of cyclin-dependent kinase 4/6, demonstrates inhibition of proliferation in renal cell carcinoma at nanomolar concentrations and molecular markers predict for sensitivity. *Anticancer Res, 33*(8), 2997-3004.
Lub, S., Maes, K., Menu, E., Bruyne, E., Vanderkerken, K., & Valckenborgh, E. V. (2015). Novel strategies to target the ubiquitin proteasome system in multiple myeloma. *Oncotarget*. doi:10.18632/oncotarget.6658
Mahgoub, T., Eustace, A. J., Collins, D. M., Walsh, N., O'Donovan, N., & Crown, J. (2015). Kinase inhibitor screening identifies CDK4 as a potential therapeutic target for melanoma. *Int J Oncol, 47*(3), 900-908. doi:10.3892/ijo.2015.3097
Malumbres, M., Sotillo, R. O., SantamaríA, D., Galán, J., Cerezo, A., Ortega, S., Dubus, P., & Barbacid, M. (2004). Mammalian cells cycle without the D-type cyclin-dependent kinases Cdk4 and Cdk6. *Cell, 118*(4), 493-504.
Marzec, M., Kasprzycka, M., Lai, R., Gladden, A. B., Wlodarski, P., Tomczak, E., Nowell, P., Deprimo, S. E., Sadis, S., Eck, S., Schuster, S. J., Diehl, J. A., & Wasik, M. A. (2006). Mantle cell lymphoma cells express predominantly cyclin D1a isoform and are highly sensitive to selective inhibition of CDK4 kinase activity. *Blood, 108*(5), 1744-1750. doi:10.1182/blood-2006-04-016634
Menu, E., Garcia, J., Huang, X., Di Liberto, M., Toogood, P. L., Chen, I., Vanderkerken, K., & Chen-Kiang, S. (2008). A novel therapeutic combination using PD 0332991 and bortezomib: study in the 5T33MM myeloma model. *Cancer Res, 68*(14), 5519-5523. doi:10.1158/0008-5472.can-07-6404

Michaud, K., Solomon, D. A., Oermann, E., Kim, J. S., Zhong, W. Z., Prados, M. D., Ozawa, T., James, C. D., & Waldman, T. (2010). Pharmacologic inhibition of cyclin-dependent kinases 4 and 6 arrests the growth of glioblastoma multiforme intracranial xenografts. *Cancer Res, 70*(8), 3228-3238. doi:10.1158/0008-5472.can-09-4559

Miller, T. W., Balko, J. M., Fox, E. M., Ghazoui, Z., Dunbier, A., Anderson, H., Dowsett, M., Jiang, A., Smith, R. A., Maira, S. M., Manning, H. C., Gonzalez-Angulo, A. M., Mills, G. B., Higham, C., Chanthaphaychith, S., Kuba, M. G., Miller, W. R., Shyr, Y., & Arteaga, C. L. (2011). ERalpha-dependent E2F transcription can mediate resistance to estrogen deprivation in human breast cancer. *Cancer Discov, 1*(4), 338-351. doi:10.1158/2159-8290.cd-11-0101

Mok, T. S., Wu, Y. L., Thongprasert, S., Yang, C. H., Chu, D. T., Saijo, N., Sunpaweravong, P., Han, B., Margono, B., Ichinose, Y., Nishiwaki, Y., Ohe, Y., Yang, J. J., Chewaskulyong, B., Jiang, H., Duffield, E. L., Watkins, C. L., Armour, A. A., & Fukuoka, M. (2009). Gefitinib or carboplatin-paclitaxel in pulmonary adenocarcinoma. *N Engl J Med, 361*(10), 947-957. doi:10.1056/NEJMoa0810699

Moll, U. M., & Petrenko, O. (2003). The MDM2-p53 interaction. *Mol Cancer Res, 1*(14), 1001-1008.

Muncaster, M. M., Cohen, B. L., Phillips, R. A., & Gallie, B. L. (1992). Failure of RB1 to reverse the malignant phenotype of human tumor cell lines. *Cancer Res, 52*(3), 654-661.

Munger, K., Basile, J. R., Duensing, S., Eichten, A., Gonzalez, S. L., Grace, M., & Zacny, V. L. (2001). Biological activities and molecular targets of the human papillomavirus E7 oncoprotein. *Oncogene, 20*(54), 7888-7898. doi:10.1038/sj.onc.1204860

Narasimha, A. M., Kaulich, M., Shapiro, G. S., Choi, Y. J., Sicinski, P., & Dowdy, S. F. (2014). Cyclin D activates the Rb tumor suppressor by mono-phosphorylation. *Elife, 3*. doi:10.7554/eLife.02872

Netto, G. J. (2016). Role for anti-PD-L1 immune checkpoint inhibitor in advanced urothelial carcinoma. *Lancet, 387*(10031), 1881-1882. doi:10.1016/s0140-6736(16)00654-1

Olanich, M. E., Sun, W., Hewitt, S. M., Abdullaev, Z., Pack, S. D., & Barr, F. G. (2015). CDK4 Amplification Reduces Sensitivity to CDK4/6 Inhibition in Fusion-Positive Rhabdomyosarcoma. *Clin Cancer Res, 21*(21), 4947-4959. doi:10.1158/1078-0432.ccr-14-2955

Pan, Q., Sathe, A., Black, P. C., Goebell, P. J., Kamat, A. M., Schmitz-Draeger, B., & Nawroth, R. (2017). CDK4/6 Inhibitors in Cancer Therapy: A Novel Treatement Strategy for Bladder Cancer. *Bladder Cancer, 3*(2), 79-88. doi:10.3233/blc-170105

Park, S., Lee, J., Do, I. G., Jang, J., Rho, K., Ahn, S., Maruja, L., Kim, S. J., Kim, K. M., Mao, M., Oh, E., Kim, Y. J., Kim, J., & Choi, Y. L. (2014). Aberrant CDK4 amplification in refractory rhabdomyosarcoma as identified by genomic profiling. *Sci Rep, 4*, 3623. doi:10.1038/srep03623

Patnaik, A., Rosen, L. S., Tolaney, S. M., Tolcher, A. W., Goldman, J. W., Gandhi, L., Papadopoulos, K. P., Beeram, M., Rasco, D. W., Hilton, J. F., Nasir, A., Beckmann, R. P., Schade, A. E., Fulford, A. D., Nguyen, T. S., Martinez, R., Kulanthaivel, P., Li, L. Q., Frenzel, M., Cronier, D. M., Chan, E. M., Flaherty, K. T., Wen, P. Y., & Shapiro, G. I. (2016). Efficacy and Safety of Abemaciclib, an Inhibitor of CDK4 and CDK6, for Patients with Breast Cancer, Non-Small Cell Lung Cancer, and Other Solid Tumors. *Cancer Discov, 6*(7), 740-753. doi:10.1158/2159-8290.cd-16-0095

Perez, M., Munoz-Galvan, S., Jimenez-Garcia, M. P., Marin, J. J., & Carnero, A. (2015a). Efficacy of CDK4 inhibition against sarcomas depends on their levels of CDK4 and p16ink4 mRNA. *Oncotarget*. doi:10.18632/oncotarget.5829

Perez, M., Munoz-Galvan, S., Jimenez-Garcia, M. P., Marin, J. J., & Carnero, A. (2015b). Efficacy of CDK4 inhibition against sarcomas depends on their levels of CDK4 and p16ink4 mRNA. *Oncotarget, 6*(38), 40557-40574. doi:10.18632/oncotarget.5829

Peyressatre, M., Prevel, C., Pellerano, M., & Morris, M. C. (2015). Targeting cyclin-dependent kinases in human cancers: from small molecules to Peptide inhibitors. *Cancers (Basel), 7*(1), 179-237. doi:10.3390/cancers7010179

Pomerantz, J., Schreiber-Agus, N., Liegeois, N. J., Silverman, A., Alland, L., Chin, L., Potes, J., Chen, K., Orlow, I., Lee, H. W., Cordon-Cardo, C., & DePinho, R. A. (1998). The Ink4a tumor suppressor gene product, p19Arf, interacts with MDM2 and neutralizes MDM2's inhibition of p53. *Cell, 92*(6), 713-723.

Puyol, M., Martin, A., Dubus, P., Mulero, F., Pizcueta, P., Khan, G., Guerra, C., Santamaria, D., & Barbacid, M. (2010). A synthetic lethal interaction between K-Ras oncogenes and Cdk4 unveils a therapeutic strategy for non-small cell lung carcinoma. *Cancer Cell, 18*(1), 63-73. doi:10.1016/j.ccr.2010.05.025

Rader, J., Russell, M. R., Hart, L. S., Nakazawa, M. S., Belcastro, L. T., Martinez, D., Li, Y., Carpenter, E. L., Attiyeh, E. F., Diskin, S. J., Kim, S., Parasuraman, S., Caponigro, G., Schnepp, R. W., Wood, A. C., Pawel, B., Cole, K. A., & Maris, J. M. (2013). Dual CDK4/CDK6 inhibition induces cell-cycle arrest and senescence in neuroblastoma. *Clin Cancer Res, 19*(22), 6173-6182. doi:10.1158/1078-0432.ccr-13-1675

Richie, J. P., Bono, A., Denis, L. J., Jewett, M. A., Kakizoe, T., Kotake, T., Shirai, T., & Ten Kate, F. J. (1998). Tumor, nodes, metastasis (TNM) classification of bladder cancer. *Urol Oncol, 4*(4-5), 90-93.

Rivadeneira, D. B., Mayhew, C. N., Thangavel, C., Sotillo, E., Reed, C. A., Grana, X., & Knudsen, E. S. (2010). Proliferative suppression by CDK4/6 inhibition: complex function of the retinoblastoma pathway in liver tissue and hepatoma cells. *Gastroenterology, 138*(5), 1920-1930. doi:10.1053/j.gastro.2010.01.007

Salmon, P., & Trono, D. (2007). Production and titration of lentiviral vectors. *Curr Protoc Hum Genet, Chapter 12*, Unit 12 10. doi:10.1002/0471142905.hg1210s54

Sanli, O., Dobruch, J., Knowles, M. A., Burger, M., Alemozaffar, M., Nielsen, M. E., & Lotan, Y. (2017). Bladder cancer. *Nat Rev Dis Primers, 3*, 17022. doi:10.1038/nrdp.2017.22

Sarbassov, D. D., Guertin, D. A., Ali, S. M., & Sabatini, D. M. (2005). Phosphorylation and regulation of Akt/PKB by the rictor-mTOR complex. *Science, 307*(5712), 1098-1101. doi:10.1126/science.1106148

Sathe, A., Koshy, N., Schmid, S. C., Thalgott, M., Schwarzenbock, S. M., Krause, B. J., Holm, P. S., Gschwend, J. E., Retz, M., & Nawroth, R. (2015). CDK4/6-inhibition controls proliferation of bladder cancer and transcription of RB1. *J Urol*. doi:10.1016/j.juro.2015.08.082

Satyanarayana, A., & Kaldis, P. (2009). Mammalian cell-cycle regulation: several Cdks, numerous cyclins and diverse compensatory mechanisms. *Oncogene, 28*(33), 2925-2939. doi:10.1038/onc.2009.170

Sawai, C. M., Freund, J., Oh, P., Ndiaye-Lobry, D., Bretz, J. C., Strikoudis, A., Genesca, L., Trimarchi, T., Kelliher, M. A., Clark, M., Soulier, J., Chen-Kiang, S., & Aifantis, I. (2012). Therapeutic targeting of the cyclin D3:CDK4/6 complex in T cell leukemia. *Cancer Cell, 22*(4), 452-465. doi:10.1016/j.ccr.2012.09.016

Schlisio, S., Halperin, T., Vidal, M., & Nevins, J. R. (2002). Interaction of YY1 with E2Fs, mediated by RYBP, provides a mechanism for specificity of E2F function. *EMBO J, 21*(21), 5775-5786.

Sdek, P., Ying, H., Chang, D. L., Qiu, W., Zheng, H., Touitou, R., Allday, M. J., & Xiao, Z. X. (2005). MDM2 promotes proteasome-dependent ubiquitin-independent degradation of retinoblastoma protein. *Mol Cell, 20*(5), 699-708.

doi:10.1016/j.molcel.2005.10.017
Sdek, P., Ying, H., Zheng, H., Margulis, A., Tang, X., Tian, K., & Xiao, Z. X. (2004). The central acidic domain of MDM2 is critical in inhibition of retinoblastoma-mediated suppression of E2F and cell growth. *J Biol Chem, 279*(51), 53317-53322. doi:10.1074/jbc.M406062200
Serrano, M., Lin, A. W., McCurrach, M. E., Beach, D., & Lowe, S. W. (1997). Oncogenic ras provokes premature cell senescence associated with accumulation of p53 and p16INK4a. *Cell, 88*(5), 593-602.
Sherr, C. J., & Roberts, J. M. (1999). CDK inhibitors: positive and negative regulators of G1-phase progression. *Genes Dev, 13*(12), 1501-1512.
Sledge, G. W., Jr., Toi, M., Neven, P., Sohn, J., Inoue, K., Pivot, X., Burdaeva, O., Okera, M., Masuda, N., Kaufman, P. A., Koh, H., Grischke, E. M., Frenzel, M., Lin, Y., Barriga, S., Smith, I. C., Bourayou, N., & Llombart-Cussac, A. (2017). MONARCH 2: Abemaciclib in Combination With Fulvestrant in Women With HR+/HER2- Advanced Breast Cancer Who Had Progressed While Receiving Endocrine Therapy. *J Clin Oncol, 35*(25), 2875-2884. doi:10.1200/jco.2017.73.7585
Tao, Z., Le Blanc, J. M., Wang, C., Zhan, T., Zhuang, H., Wang, P., Yuan, Z., & Lu, B. (2016). Coadministration of Trametinib and Palbociclib Radiosensitizes KRAS-Mutant Non-Small Cell Lung Cancers In Vitro and In Vivo. *Clin Cancer Res, 22*(1), 122-133. doi:10.1158/1078-0432.ccr-15-0589
Tashiro, E., Tsuchiya, A., & Imoto, M. (2007). Functions of cyclin D1 as an oncogene and regulation of cyclin D1 expression. *Cancer Sci, 98*(5), 629-635. doi:10.1111/j.1349-7006.2007.00449.x
Tate, S. C., Cai, S., Ajamie, R. T., Burke, T., Beckmann, R. P., Chan, E. M., De Dios, A., Wishart, G. N., Gelbert, L. M., & Cronier, D. M. (2014). Semi-mechanistic pharmacokinetic/pharmacodynamic modeling of the antitumor activity of LY2835219, a new cyclin-dependent kinase 4/6 inhibitor, in mice bearing human tumor xenografts. *Clin Cancer Res, 20*(14), 3763-3774. doi:10.1158/1078-0432.ccr-13-2846
Taylor, B., Weinstein, J. N., Akbani, R., Broom, B. M., Wang, W., Verhaak, R. G. W., McConkey, D., Lerner, S., Morgan, M., Creighton, C. J., & Smith, C. (2014). Comprehensive molecular characterization of urothelial bladder carcinoma. *Nature, 507*(7492), 315-322. doi:10.1038/nature12965
Torre, L. A., Bray, F., Siegel, R. L., Ferlay, J., Lortet-Tieulent, J., & Jemal, A. (2015). Global cancer statistics, 2012. *CA Cancer J Clin, 65*(2), 87-108. doi:10.3322/caac.21262
Tsubuki, S., Saito, Y., Tomioka, M., Ito, H., & Kawashima, S. (1996). Differential inhibition of calpain and proteasome activities by peptidyl aldehydes of di-leucine and tri-leucine. *J Biochem, 119*(3), 572-576.
Uchida, C., Miwa, S., Kitagawa, K., Hattori, T., Isobe, T., Otani, S., Oda, T., Sugimura, H., Kamijo, T., Ookawa, K., Yasuda, H., & Kitagawa, M. (2005). Enhanced Mdm2 activity inhibits pRB function via ubiquitin-dependent degradation. *EMBO J, 24*(1), 160-169. doi:10.1038/sj.emboj.7600486
Valeriote, F., & van Putten, L. (1975). Proliferation-dependent cytotoxicity of anticancer agents: a review. *Cancer Res, 35*(10), 2619-2630.
Vieira, A. R., Vingeliene, S., Chan, D. S., Aune, D., Abar, L., Navarro Rosenblatt, D., Greenwood, D. C., & Norat, T. (2015). Fruits, vegetables, and bladder cancer risk: a systematic review and meta-analysis. *Cancer Med, 4*(1), 136-146. doi:10.1002/cam4.327
von Witzleben, A., Goerttler, L. T., Marienfeld, R., Barth, H., Lechel, A., Mellert, K., Bohm, M., Kornmann, M., Mayer-Steinacker, R., von Baer, A., Schultheiss, M., Flanagan, A.

M., Moller, P., Bruderlein, S., & Barth, T. F. (2015). Preclinical Characterization of Novel Chordoma Cell Systems and Their Targeting by Pharmocological Inhibitors of the CDK4/6 Cell-Cycle Pathway. *Cancer Res, 75*(18), 3823-3831. doi:10.1158/0008-5472.can-14-3270

Vora, S. R., Juric, D., Kim, N., Mino-Kenudson, M., Huynh, T., Costa, C., Lockerman, E. L., Pollack, S. F., Liu, M., Li, X., Lehar, J., Wiesmann, M., Wartmann, M., Chen, Y., Cao, Z. A., Pinzon-Ortiz, M., Kim, S., Schlegel, R., Huang, A., & Engelman, J. A. (2014). CDK 4/6 inhibitors sensitize PIK3CA mutant breast cancer to PI3K inhibitors. *Cancer Cell, 26*(1), 136-149. doi:10.1016/j.ccr.2014.05.020

Wang, L., Wang, J., Blaser, B. W., Duchemin, A. M., Kusewitt, D. F., Liu, T., Caligiuri, M. A., & Briesewitz, R. (2007). Pharmacologic inhibition of CDK4/6: mechanistic evidence for selective activity or acquired resistance in acute myeloid leukemia. *Blood, 110*(6), 2075-2083. doi:10.1182/blood-2007-02-071266

Wang, Y., Zheng, Z., Zhang, J., Kong, R., Liu, J., Zhang, Y., Deng, H., Du, X., & Ke, Y. (2015). A Novel Retinoblastoma Protein (RB) E3 Ubiquitin Ligase (NRBE3) Promotes RB Degradation and Is Transcriptionally Regulated by E2F1 Transcription Factor. *J Biol Chem, 290*(47), 28200-28213. doi:10.1074/jbc.M115.655597

Wiedemeyer, W. R., Dunn, I. F., Quayle, S. N., Zhang, J., Chheda, M. G., Dunn, G. P., Zhuang, L., Rosenbluh, J., Chen, S., Xiao, Y., Shapiro, G. I., Hahn, W. C., & Chin, L. (2010). Pattern of retinoblastoma pathway inactivation dictates response to CDK4/6 inhibition in GBM. *Proc Natl Acad Sci U S A, 107*(25), 11501-11506. doi:10.1073/pnas.1001613107

Witjes, J. A., Comperat, E., Cowan, N. C., De Santis, M., Gakis, G., Lebret, T., Ribal, M. J., Van der Heijden, A. G., & Sherif, A. (2014). EAU guidelines on muscle-invasive and metastatic bladder cancer: summary of the 2013 guidelines. *Eur Urol, 65*(4), 778-792. doi:10.1016/j.eururo.2013.11.046

Witkiewicz, A. K., Borja, N. A., Franco, J., Brody, J. R., Yeo, C. J., Mansour, J., Choti, M. A., McCue, P., & Knudsen, E. S. (2015). Selective impact of CDK4/6 suppression on patient-derived models of pancreatic cancer. *Oncotarget, 6*(18), 15788-15801.

Witkiewicz, A. K., Cox, D., & Knudsen, E. S. (2014). CDK4/6 inhibition provides a potent adjunct to Her2-targeted therapies in preclinical breast cancer models. *Genes Cancer, 5*(7-8), 261-272.

Witkiewicz, A. K., Knudsen, K. E., Dicker, A. P., & Knudsen, E. S. (2011). The meaning of p16(ink4a) expression in tumors: functional significance, clinical associations and future developments. *Cell Cycle, 10*(15), 2497-2503.

Wu, L., Timmers, C., Maiti, B., Saavedra, H. I., Sang, L., Chong, G. T., Nuckolls, F., Giangrande, P., Wright, F. A., Field, S. J., Greenberg, M. E., Orkin, S., Nevins, J. R., Robinson, M. L., & Leone, G. (2001). The E2F1-3 transcription factors are essential for cellular proliferation. *Nature, 414*(6862), 457-462. doi:10.1038/35106593

Xiao, Z. X., Chen, J., Levine, A. J., Modjtahedi, N., Xing, J., Sellers, W. R., & Livingston, D. M. (1995). Interaction between the retinoblastoma protein and the oncoprotein MDM2. *Nature, 375*(6533), 694-698. doi:10.1038/375694a0

Yadav, V., Burke, T. F., Huber, L., Van Horn, R. D., Zhang, Y., Buchanan, S. G., Chan, E. M., Starling, J. J., Beckmann, R. P., & Peng, S. B. (2014). The CDK4/6 inhibitor LY2835219 overcomes vemurafenib resistance resulting from MAPK reactivation and cyclin D1 upregulation. *Mol Cancer Ther, 13*(10), 2253-2263. doi:10.1158/1535-7163.mct-14-0257

Yang, C., Li, Z., Bhatt, T., Dickler, M., Giri, D., Scaltriti, M., Baselga, J., Rosen, N., & Chandarlapaty, S. (2016). Acquired CDK6 amplification promotes breast cancer resistance to CDK4/6 inhibitors and loss of ER signaling and dependence.

Oncogene. doi:10.1038/onc.2016.379
Ying, H., & Xiao, Z. X. (2006). Targeting retinoblastoma protein for degradation by proteasomes. *Cell Cycle, 5*(5), 506-508. doi:10.4161/cc.5.5.2515
Yoshida, A., Lee, E. K., & Diehl, J. A. (2016). Induction of Therapeutic Senescence in Vemurafenib-Resistant Melanoma by Extended Inhibition of CDK4/6. *Cancer Res, 76*(10), 2990-3002. doi:10.1158/0008-5472.can-15-2931
Young, R. J., Waldeck, K., Martin, C., Foo, J. H., Cameron, D. P., Kirby, L., Do, H., Mitchell, C., Cullinane, C., Liu, W., Fox, S. B., Dutton-Regester, K., Hayward, N. K., Jene, N., Dobrovic, A., Pearson, R. B., Christensen, J. G., Randolph, S., McArthur, G. A., & Sheppard, K. E. (2014). Loss of CDKN2A expression is a frequent event in primary invasive melanoma and correlates with sensitivity to the CDK4/6 inhibitor PD0332991 in melanoma cell lines. *Pigment Cell Melanoma Res, 27*(4), 590-600. doi:10.1111/pcmr.12228
Zhang, Y. X., Sicinska, E., Czaplinski, J. T., Remillard, S. P., Moss, S., Wang, Y., Brain, C., Loo, A., Snyder, E. L., Demetri, G. D., Kim, S., Kung, A. L., & Wagner, A. J. (2014). Antiproliferative effects of CDK4/6 inhibition in CDK4-amplified human liposarcoma in vitro and in vivo. *Mol Cancer Ther, 13*(9), 2184-2193. doi:10.1158/1535-7163.mct-14-0387

Publication

Pan, Q., A. Sathe, et al. (2017). "CDK4/6 Inhibitors in Cancer Therapy: A Novel Treatement Strategy for Bladder Cancer." Bladder Cancer 3(2): 79-88.